REVIEW

Check for updates

Factors governing tumor penetration of nanomedicines: intrinsic and extrinsic determinants

Dongwon Shin, ID †[a,b] Jiwoong Choi,†[c] Byeongmin Park,[a,b] Sun Hwa Kim ID *[a,b] and Man Kyu Shim ID *[b]

Nanomedicine-based drug delivery has shown considerable promise for cancer therapy; however, the efficient transport and deep penetration of nanoparticles within solid tumors remain major challenges for clinical translation. These limitations arise from the combined effects of nanoparticle physicochemical properties and biological transport barriers acting across multiple biological scales, rather than being governed by any single isolated parameter. Accordingly, nanoparticle transport and tumor penetration cannot be adequately understood by considering individual parameters in isolation, but instead reflect the combined contributions of intrinsic determinants related to nanoparticle properties and extrinsic determinants associated with penetration-enhancing interventions, underscoring the need for an integrated framework that explicitly distinguishes and organizes these two classes of factors when evaluating nanoparticle transport *in vivo*. In this review, we provide a structured overview of the intrinsic and extrinsic determinants that regulate nanoparticle transport *in vivo*. First, we summarize intrinsic nanoparticle-related factors and discuss how their physicochemical properties influence key transport processes, including systemic circulation, tumor accumulation and penetration, cellular uptake, and excretion. Second, we review advanced engineering strategies designed to enhance tissue penetration, such as size- and charge-transformable nanoplatforms that aim to balance prolonged circulation with improved intratumoral distribution. Third, we outline extrinsic intervention-based approaches, including external stimuli and pharmacological modulators, that improve nanoparticle penetration by modulating transport barriers within solid tumors. Finally, we discuss remaining challenges and knowledge gaps that limit the predictability and reproducibility of nanoparticle transport *in vivo*, and provide perspectives on how a systems-level understanding of these interdependent factors can support the clinical translation of nanomedicines.

1. Introduction

Nanoparticles have been extensively integrated into diagnostic platforms, imaging tools, and therapeutic agents to enable early detection and more effective disease management.[1,2] A thorough understanding of their behavior within the body is essential for designing nanomedicines with optimized targeting, absorption, and clearance profiles, as well as for ensuring successful clinical translation.[3] Among the various factors influencing nanoparticle transport, particle size stands out

[a]KU-KIST Graduate School of Converging Science and Technology, Korea University, Seoul 02841, Republic of Korea. E-mail: sunkim@kist.re.kr, mks@kist.re.kr
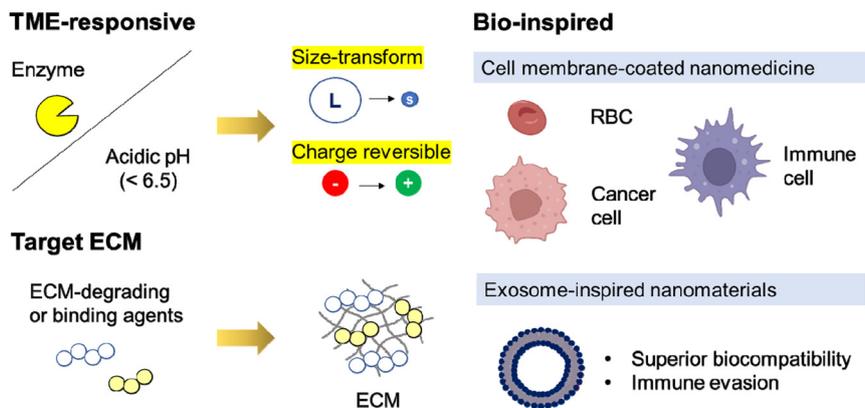*[b]Medicinal Materials Research Center, Biomedical Research Division, Korea Institute of Science and Technology (KIST), Seoul 02792, Republic of Korea*
[c]Department of Immunology, School of Medicine, Kyungpook National University, Daegu, 41944, Republic of Korea
† These authors contributed equally to this work.

because many physiological barriers impose distinct dimensional limits.[4] For instance, normal capillaries possess endothelial gaps of approximately 10 nm, whereas tumor blood vessels often exhibit enlarged openings exceeding 50 nm.[5,6] These structural size variations allow appropriately sized nanoparticles to preferentially accumulate in tumor tissues, improving targeting efficiency while minimizing off-target distribution.[7,8] Furthermore, numerous nano-bio interactions, such as cellular internalization, are highly sensitive to particle dimensions, further supporting the strategic use of size for selective tumor delivery.[9]

Upon entry into the body, nanoparticle behavior is influenced not only by size but also by a range of physicochemical properties and biological factors.[10] In particular, tumor penetration is strongly dependent on characteristics such as surface charge, stiffness, morphology, and composition.[11] To address these challenges, various engineered nanomedicines have been developed, including platforms with stimuli-responsive
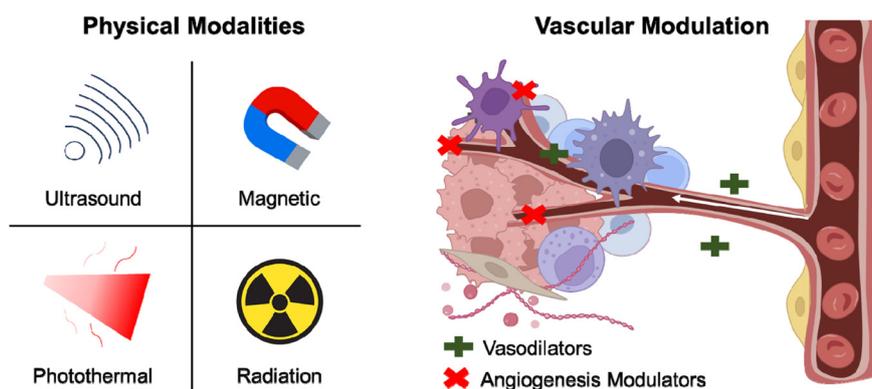
Fig. 1 Schematic illustration of intrinsic and extrinsic factors governing tumor penetration of nanomedicines.

Dongwon Shin is a combined M. S.-Ph.D. candidate at the KU-KIST Graduate School of Converging Science and Technology, Korea University. He is also a student trainee at the Korea Institute of Science and Technology (KIST). Under the supervision of his advisors, his research focuses on the design of supramolecular self-assembly-based therapeutics and the development of nanomedicine drug delivery systems.

Dongwon Shin

Jiwoong Choi is an Assistant Professor in the Department of Immunology, School of Medicine, Kyungpook National University (KNU), Korea. His current research focuses on developing innovative peptide- and nanomedicine-based drug delivery platforms to enhance therapeutic efficacy and precision in immunotherapy. By integrating principles of nanomedicine, advanced drug delivery, and immuno-oncology, his work aims to overcome key biological barriers and expand translational opportunities for next-generation immune-modulating therapies.

Jiwoong Choi

size or charge switching, bio-inspired surface modifications, and extracellular matrix targeting functionalities.[12–15] These strategies are designed to preserve favorable circulation and tumor targeting while enhancing penetration into tumor tissues. In addition, abnormal features of the tumor microenvironment, such as dense extracellular matrix, elevated interstitial pressure, and irregular vasculature, can substantially hinder nanoparticle transport.[16,17] As a result, pharmacological and physical interventions have been explored to transiently modulate the tumor microenvironment and improve nanoparticle penetration.

This review aims to provide a comprehensive understanding of the intrinsic and extrinsic factors influencing nanoparticle tumor penetration from three major perspectives: (i) the intrinsic properties of nanomedicines, (ii) advanced engineering strategies to enhance tissue penetration, and (iii) external stimuli and pharmacological modulators (Fig. 1). By distinguishing intrinsic nanoparticle-related determinants from extrinsic intervention-based strategies that modulate tumor penetration, this organizational framework allows recent advances in nanotherapeutic design and penetration-enhancing approaches to be discussed. Accordingly, we highlight recent progress in the rational design of nanotherapeutic strategies to achieve deep tumor penetration and further discuss perspectives in this challenging field. Based on these summaries and analyses, the review offers practical directions to translate the potential of nanomedicine into patient benefit.

2. Intrinsic physicochemical properties

The intrinsic physicochemical properties of nanomedicines, including size, surface charge, deformability, shape, and material composition, are the fundamental parameters that determine their *in vivo* pharmacokinetic and tissue distribution profiles (Fig. 2).[18–20] The rational design of these properties is crucial for navigating the complex biological barriers of the tumor microenvironment and achieving effective tumor

penetration. These properties govern how nanoparticles traverse the abnormal vasculature, diffuse through the dense extracellular matrix, and interact with tumor and stromal cells. Optimal tuning of these parameters enables deep and uniform penetration into tumor cores, overcoming perivascular accumulation and heterogeneous drug distribution that often limit therapeutic efficacy.

2.1. Size

The size of nanomedicines is a primary determinant of its *in vivo* fate, presenting conflicting requirements for systemic circulation *versus* deep tissue penetration. From a pharmacokinetic and biodistribution standpoint, nanoparticles with relatively larger hydrodynamic diameters tend to exhibit superior systemic persistence and more pronounced initial tumor accumulation. Nanomedicines with diameters in the range of 50–200 nm are well-suited to avoid both rapid renal filtration, which predominantly eliminates objects smaller than about 10 nm, and premature removal by the reticuloendothelial system (RES), resulting in longer circulation times and higher accumulation in tumor tissues *via* the enhanced permeability and retention (EPR) effect.[21–25] Despite this superior accumulation, the larger size of these nanomedicines becomes a significant barrier to effective therapy, as they exhibit minimal penetration beyond the perivascular regions of the tumor and become lodged in the dense extracellular matrix.

Conversely, for effective penetration deep into the tumor, smaller nanomedicines are advantageous. Nanomedicines with diameters less than 30 nm are known to navigate the tortuous interstitial spaces of the dense tumor parenchyma more effectively, leading to a more uniform drug distribution.[26] This enhanced penetration can result in comparable therapeutic efficacy to larger particles, even with lower initial tumor accumulation. However, this advantage in penetration is often offset by their rapid systemic clearance, which diminishes the total dose that accumulates at the tumor site.[27] This inverse relationship between the optimal size for circulation and that for penetration establishes a fundamental challenge in nanomedicine design, necessitating advanced strategies such as size-transformable nanosystems.

2.2. Surface charge

Surface charge is another critical parameter that profoundly influences the *in vivo* behavior of nanomedicines, creating conflicting requirements for systemic stability and intratumoral activity. For optimal systemic circulation, nanoparticles with neutral or slightly anionic surface potentials are preferred, as these surfaces minimize nonspecific protein adsorption and opsonization, thereby reducing macrophage recognition and clearance by the mononuclear phagocyte system (MPS) while prolonging blood circulation time.[28,29]

However, within the TME, a positive surface charge often confers therapeutic advantages. In early studies, the enhanced cellular uptake and tumor penetration of positively charged nanomedicines were largely attributed to electrostatic interactions with negatively charged cell membranes and the extra-

Man Kyu Shim is a Senior Research Scientist at the Korea Institute of Science and Technology (KIST), affiliated with the Medicinal Materials Research Center, and also serves as an Associate Professor at the University of Science and Technology, Republic of Korea. His research centers on nanomedicine, with an emphasis on designing supramolecular drug delivery systems for therapeutic applications.
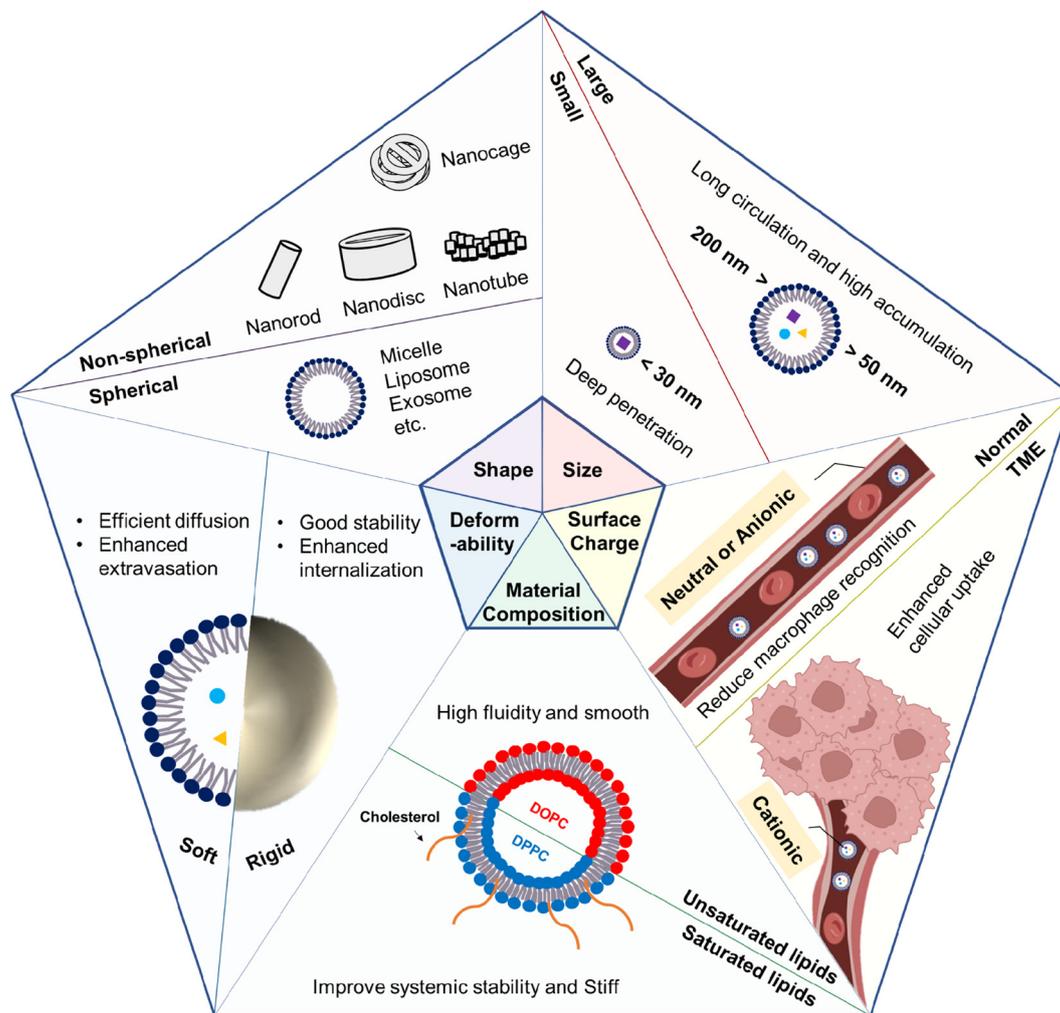
Man Kyu Shim

Fig. 2 Intrinsic physicochemical determinants of nanomedicine tumor penetration.

cellular matrix (ECM).[30] Several studies have reported that cationic nanoparticles can achieve superior antitumor efficacy compared to their neutral or anionic counterparts, an effect attributed not to higher tumor deposition, but to significantly improved penetration and cellular accumulation.[12,31,32] Conversely, accumulating evidence indicates that cellular internalization and intratumoral tissue penetration are not necessarily coupled and may, under certain conditions, exhibit an inverse relationship.[33] Nanoparticles with strong electrostatic affinity for the plasma membrane can be rapidly captured and internalized by perivascular cells, which reduces the freely diffusible fraction and limits onward transport into the tumor interior.[34] By contrast, nanocarriers engineered to attenuate nonspecific membrane interactions typically display greater interstitial mobility, enabling deeper distribution throughout the tumor parenchyma.

Furthermore, current consensus suggests a more complex scenario in physiological environments. Upon exposure to biological fluids, nanoparticles rapidly acquire a layer of biomolecules, known as the 'protein corona,' which defines their biological identity.[35,36] This corona forms on the nanoparticle surface in a charge-dependent manner, dictating subsequent interactions within the TME.[37] Consequently, the surface charge of the bare nanoparticle may not interact directly with the cell membrane. Instead, the initial positive charge plays a critical role in determining the composition of the protein corona, potentially enriching it with specific proteins that facilitate receptor-mediated endocytosis, thereby mediating the high cellular uptake often observed with cationic carriers.

2.3. Deformability

The mechanical properties of nanomedicines, specifically their deformability and rigidity, are critical factors that influence their therapeutic efficacy by governing both tumor penetration and systemic circulation.[38] Soft and highly deformable nanomedicines possess a distinct advantage in traversing the dense TME, as their dynamic shape adaptability enables them to pass through narrow intercellular junctions and compact extracellular matrices, thereby facilitating efficient diffusion and deep tumor penetration.[39] This has been consistently

observed in various *in vitro* models, such as 3D multicellular spheroids, where soft nanogels and nanomicelles with soft cores demonstrate significantly greater permeability compared to their rigid counterparts.[40] This superior penetration capability extends to *in vivo* settings, where soft nanomedicines show enhanced extravasation from tumor blood vessels and a more uniform distribution throughout the tumor tissue.

Conversely, a more rigid structure can confer advantages in other aspects of drug delivery. A stiffer nanoparticle can offer greater colloidal stability during circulation and influence the dynamics of cellular uptake.[41] Some reports suggest that stiffer nanoparticles are internalized more readily by certain cancer cell types, potentially due to lower energy penalties associated with membrane wrapping during endocytosis.[42] However, this same rigidity severely limits their ability to move through the tumor interstitium after extravasation. Interestingly, some studies indicate that intermediate stiffness or semi-elastics may be optimal both softer and harder equivalents in tumor penetration.[43] This suggests that the relationship between mechanical properties and penetration is complex and may be tumor-type dependent. Therefore, the deformability of a nanocarrier can be precisely engineered by modulating its material composition allowing for a tailored approach to balance the conflicting demands of circulation stability, cellular uptake, and deep tumor penetration.

2.4. Shape

The geometrical properties of a nanomedicine are another important factor in determining not only its deep tissue penetration into tumors but also its systemic circulation and vascular extravasation.[44,45] Although spherical nanomedicines have been the most widely investigated, largely because spherical morphology is the most thermodynamically stable outcome of many self-assembly and synthesis methods, non-spherical designs can offer distinct advantages for tumor penetration. For example, nanomedicines engineered with various non-spherical shapes, such as nanorods,[46,47] nanodiscs,[48,49] nanotubes,[50,51] nanocages,[52,53] and filamentous micelles,[54,55] exhibit distinct transport behaviors that can be leveraged for improved therapeutic outcomes. These alternative geometries exhibit more complex rotational and translational dynamics within blood flow, promoting enhanced margination toward the vessel wall and thereby increasing the likelihood of extravasation into tumor tissues. Once within the tumor interstitium, their elongated architectures are particularly advantageous for navigating the dense and tortuous extracellular matrix, as exemplified by filamentous micelles, which leverage their high aspect ratio and flexibility to align with interstitial flow, traverse endothelial gaps more efficiently, and achieve deeper tumor penetration and prolonged circulation relative to their spherical counterparts. Notably, the aspect ratio of elongated nanomedicines is a critical determinant of their performance since studies with nanorods have demonstrated that intermediate aspect ratios maximize penetration, whereas excessively high or low ratios are less effective.[56,57] The optimal geometry, however, is not universal and varies with the nano-carrier composition and tumor type. For instance, single-walled carbon nanotubes penetrated more efficiently than spherical quantum dots in a U87MG glioblastoma model, whereas the opposite trend was observed in LS174T colorectal tumors.[58] Thus, nanomedicine shape design requires a careful balance between enhancing tumor penetration and preserving favorable circulation and biodistribution profiles.

2.5. Material composition

The selection of constituent materials is a crucial determinant for nanomedicine performance, as the material composition directly governs other intrinsic properties such as the nano-carrier's deformability, which in turn profoundly impacts tumor penetration. The interplay between lipid composition and membrane rigidity in liposomal systems serves as a prime example of this principle.[59,60] The mechanical properties of a liposome are dictated by the thermodynamic phase state of its lipid bilayer, which can be precisely controlled by the selection of its components. Liposomes formulated with unsaturated lipids, such as dioleoylphosphatidylcholine (DOPC), exist in a liquid-disordered phase. This phase is characterized by high fluidity and low lipid packing density, resulting in a soft, highly deformable nanoparticle that is well-suited to squeeze through the tight interstitial spaces of the tumor microenvironment.

Conversely, incorporating saturated lipids such as dipalmitoylphosphatidylcholine (DPPC) or adding cholesterol markedly increases membrane rigidity. Cholesterol promotes a liquid-ordered phase by tightening lipid packing, which results in stiffer and less deformable membranes.[61] Experimental measurements of the bending modulus further support this trend, showing that membranes in the solid-ordered phase are the most rigid, followed by the liquid-ordered phase, while the liquid-disordered phase remains the most flexible.[62] These findings clearly illustrate how molecular composition dictates mechanical behavior. Thus, material selection becomes a pivotal design consideration where rigid formulations improve systemic stability while fluid and deformable formulations facilitate navigation through the dense tumor matrix. Achieving optimal therapeutic outcomes requires carefully balancing these opposing needs through rational control of material composition.

Ultimately, while the intrinsic features of nanomedicines are intimately linked to their biological performance, defining a universally optimal size, charge, shape, or mechanical property remains highly challenging. This complexity arises from the heterogeneity of tumor microenvironments and the context-dependent nature of nanoparticle transport, where design parameters that favor one stage of delivery may compromise another. For instance, features that enhance systemic circulation or vascular extravasation can hinder deep tissue penetration, and *vice versa*. Moreover, the physicochemical properties that maximize therapeutic efficacy in one tumor model may not translate directly to another due to variations in vascular structure, extracellular matrix density, and interstitial fluid dynamics. Therefore, while precise engineering of material

composition and other intrinsic parameters is essential, such optimization can only partially overcome the multifaceted barriers to effective nanoparticle penetration, highlighting the need for adaptable and context-responsive design strategies.

3. Advanced engineering strategies

3.1. Tumor microenvironment-responsive strategies

The optimal physicochemical characteristics required at each stage of the delivery cascade are distinct and often conflicting, which highlights the need for transformable nanoparticles capable of adapting their properties in response to different environments.[63–65,117] Incorporating stimuli-responsive components enables nanomedicines to dynamically adjust their size or surface charge once they reach the tumor site. Such transformations are commonly triggered by the unique conditions of the tumor microenvironment, including mild acidity, redox imbalance, or the overexpression of specific enzymes.

Size-transform. Size-transformable nanomedicines have been proposed as an elegant solution to overcome the contradictory demands of systemic pharmacokinetics and intratumoral penetration. Larger nanoparticles generally exhibit prolonged circulation and enhanced tumor accumulation but are often restricted to perivascular regions, whereas smaller counterparts penetrate more deeply into tumor tissues yet suffer from rapid clearance. To address this trade-off, stimuli-responsive multistage systems have been designed to remain intact during circulation and tumor accumulation and then disassemble into smaller subunits once exposed to the unique biochemical and physical conditions of the tumor microenvironment. The released fragments are engineered to maintain colloidal stability, minimize nonspecific protein adsorption, and sustain interstitial transport, thereby achieving a more homogeneous distribution of therapeutic payloads throughout the tumor parenchyma.

The tumor microenvironment is enriched with various enzymes, such as cathepsins, matrix metalloproteinases and hyaluronidases, which can be harnessed to trigger structural transformations of nanocarriers.[66–68] Leveraging these tumor-specific enzymatic activities, several groups have designed nanoparticles that undergo size shrinkage to overcome stromal barriers and achieve deeper penetration. Wong et al. engineered a multistage delivery system in which PEGylated gelatin nanoparticles of ~100 nm encapsulated 10 nm quantum dot subunits.[69] In the tumor microenvironment, matrix metalloproteinase-2 (MMP-2), abundantly expressed in invasive carcinomas, degraded the gelatin core and released the ultrasmall quantum dots. These fragments displayed rapid diffusion through dense collagen matrices and penetrated 300 micrometers into HT-1080 fibrosarcoma xenografts, achieving markedly improved intratumoral distribution compared to non-cleavable carriers. Importantly, the system combined prolonged circulation with deep penetration, demonstrating the potential of enzyme-triggered size shrinkage for

overcoming stromal barriers. In a related strategy, Hu et al. developed dendritic prodrug of indocyanine green/doxorubicin (IDD) with a hyaluronidase-sensitive shell (IDDHN).[13] In the tumor microenvironment, hyaluronidase-mediated degradation of the hyaluronic acid coating reduced their size from 264 nm to approximately 35 nm, thereby facilitating deeper intratumoral penetration in 4T1 breast carcinoma models. This enzyme-triggered size shrinkage markedly enhanced drug distribution and antitumor efficacy.

Excessive glycolysis in tumors lowers extracellular pH to around 6.5, compared with 7.4 in normal tissues, and this acidic environment has been widely exploited for size transformation. Yang et al. designed peptide–polymer conjugates that initially self-assembled into nanoparticles of approximately 39 nm at neutral pH but transformed into β-sheet nanofibers of 6.9 nm under mildly acidic conditions.[70] This transition involved both a reduction in size and a change in morphology from spherical particles to elongated fibrous structures. In MCF-7 xenografts, the in situ – formed nanofibers persisted for more than 96 hours and acted as hosts to trap subsequently administered agents such as doxorubicin and indocyanine green through host–guest interaction, leading to complete tumor ablation under near-infrared irradiation with minimal systemic toxicity. Similarly, He et al. reported a pH-responsive size-shrinkable mesoporous silica-based nanocarrier consisting of an ultrasmall amino-functionalized mesoporous silica core (USMSN-NH2) coated with a lipid layer containing spiropyran derivatives.[14] The nanocarrier exhibited an initial hydrodynamic size of 33.41 nm, which enabled effective tumor accumulation via the EPR effect. Upon exposure to the acidic tumor microenvironment, the spiropyran underwent a hydrophobic-to-hydrophilic conversion, leading to lipid layer compaction and a size reduction to ~17 nm. This shrinkage promoted deep penetration into 4T1 tumors while also facilitating rapid systemic clearance, thereby reducing long-term toxicity. Doxorubicin-loaded formulations achieved significantly enhanced tumor inhibition and prolonged survival compared with controls, demonstrating the therapeutic potential of acid-triggered size-switchable silica nanocarriers.

The tumor intracellular environment is highly reductive due to elevated glutathione (GSH) levels, which can reach 2–10 mM compared to much lower concentrations in normal tissues. This redox gradient provides a potent trigger for disulfide bond cleavage and carrier disassembly, enabling responsive size or morphology transformation of nanomedicines. Guo et al. developed a glutathione-responsive system in which PEG–TGA–NapFFKY peptide conjugates encapsulating doxorubicin initially self-assembled into micelles size of 192 nm but underwent intracellular restructuring into one-dimensional nanofibers in response to high GSH levels.[71] This micelle-to-fiber transition markedly enhanced doxorubicin release altered tumor cell morphology and cytoskeleton, and induced apoptosis, leading to synergistic chemotherapy effects in A549 xenografts with improved biocompatibility and reduced cardiotoxicity. Similarly, Campea et al. developed disulfide-crosslinked nanogel-based nanoassemblies that encap-

sulated ultrasmall starch nanoparticles (10–40 nm) within a chondroitin sulfate-based nanogel matrix (150–250 nm).[72] In circulation, the larger assemblies provided prolonged stability, while in the reductive tumor microenvironment, the nanogels degraded to release doxorubicin-loaded starch nanoparticles. These ultrasmall fragments penetrated efficiently into CT26 colon carcinoma spheroids, achieving over an order of magnitude higher intratumoral fluorescence than free doxorubicin. *In vivo*, doxorubicin-loaded nanoassemblies suppressed tumor growth six-fold relative to saline and two-fold relative to free drug, while reducing systemic toxicity, thereby demonstrating the therapeutic potential of tumor microenvironment–responsive nanogel assemblies.

Surface charge-transform. TME–responsive charge conversion has been increasingly recognized as an effective strategy to overcome the dichotomy between circulation stability and intratumoral delivery. Nanocarriers with neutral or slightly negative surface charge exhibit prolonged blood circulation by minimizing nonspecific protein adsorption and reticuloendothelial clearance, whereas positively charged surfaces facilitate electrostatic interactions with the negatively charged tumor cell membranes and extracellular matrix, thereby enhancing cellular uptake and deep tissue penetration. Dynamic surface charge–switching systems exploit stimuli such as hypoxic, acidic pH, enzymatic cleavage, within the TME to trigger a transition from a stealth, circulation-favorable state to a cationic, penetration-competent state, thus reconciling these otherwise conflicting requirements.

Solid tumors frequently develop hypoxic regions due to abnormal vasculature and excessive oxygen consumption, creating steep oxygen gradients within the tissue. Hypoxia not only promotes tumor aggressiveness and therapeutic resistance but also provides a unique endogenous trigger that can be harnessed for responsive drug delivery systems. Chen *et al.* designed aptamer-functionalized, hypoxia-sensitive, and charge-switchable nanoparticles (s(DGL)n@Apt) that co-encapsulated gemcitabine monophosphate together with the STAT3 inhibitor HJC0152.[73] These nanoparticles circulated in a stealth, negatively charged state, but in the hypoxic pancreatic ductal adenocarcinoma (PDAC) microenvironment, the aptamer shell detached to expose a cationic core. The charge reversal enhanced tumor penetration and facilitated gemcitabine uptake, while HJC0152 suppressed STAT3 signaling, remodeled the extracellular matrix, and alleviated immunosuppression. In orthotopic PDAC models, this dual-drug system produced potent tumor inhibition and robust immune activation, underscoring the therapeutic potential of hypoxia-triggered charge conversion.

Beyond hypoxia, the mildly acidic TME is a well-established trigger for charge reversal that facilitates deeper tumor penetration. Wang *et al.* reported a metformin-modified nanohybrid (Met@BF) incorporating Fe_3O_4 and $BaTiO_3$ cores with a Met-DSPE-PEG shell.[74] The system remained negatively charged during systemic circulation but underwent rapid charge conversion to a positive state in the acidic TME, which significantly enhanced deep tumor penetration. Under ultrasound irradiation, $BaTiO_3$ mediated piezocatalysis to generate H_2O_2, which synergistically amplified Fe_3O_4-mediated Fenton chemistry for robust ROS production. Concurrently, metformin release suppressed PD-L1 expression, reprogramming the immune microenvironment and boosting T-cell activity. In melanoma models, this multifunctional strategy effectively inhibited both primary and metastatic tumors, highlighting the therapeutic synergy of pH-triggered charge conversion with piezo-augmented chemodynamic and immunotherapy. In a related approach, Liu *et al.* constructed hierarchically stimuli-responsive nanovectors based on hollow mesoporous silica nanoparticles (HMSNs, ~120 nm) complexed with a platinum (IV) prodrug–conjugated PAMAM dendrimer (~5 nm).[75] To endow pH sensitivity, the HMSNs were functionalized with dimethylmaleic anhydride–modified chitosan, which enabled charge reversal under mildly acidic conditions. In circulation, the system remained stable and negatively charged, favoring prolonged blood circulation and EPR-mediated accumulation. Once in the tumor microenvironment, acid-triggered charge reversal caused the disassembly of the complex into HMSN@GEM carriers and ultrasmall PAMAM-Pt dendrimers. The latter, with their small size and positive charge, penetrated deeply into multicellular spheroids and tumor parenchyma, while intracellular reductive conditions further activated the Pt prodrug. This dual-stage system achieved nearly complete suppression of A549 xenografts and extended mouse survival, underscoring the power of pH-mediated charge conversion to coordinate systemic stability with deep tumor penetration.

In contrast, Dai *et al.* exploited a tumor-specific enzyme to achieve charge reversal.[76] They designed a library of modular peptides as surface ligands for CdSe/ZnS quantum dots (QDs), incorporating γ-glutamyl transpeptidase (GGT)–cleavable motifs. In circulation, the peptide-coated QDs remained zwitterionic and negatively charged, minimizing nonspecific interactions. Upon encountering overexpressed GGT on tumor cell membranes, the γ-glutamyl bond was hydrolyzed, exposing protonated amino groups and thereby converting the surface charge from negative to positive. This enzyme-triggered charge reversal significantly enhanced endocytosis in GGT-positive tumor cells and enabled deeper penetration into multicellular spheroids, compared to non-cleavable controls. These findings highlight GGT-responsive peptide ligands as a promising strategy for tumor-specific activation of charge-switchable nanomedicines (Table 1).

3.2. Bio-inspired strategies

Bio-inspired strategies leverage design principles derived from biological systems to enhance the performance of nanomedicines. By mimicking the structural or functional attributes of natural entities such as cell membranes and extracellular vesicles, these approaches endow synthetic nanocarriers with superior biocompatibility, immune evasion, and deep tumor penetration.

Cell membrane-coated nanomedicine. The cancer cell membrane is enriched with adhesion molecules and surface ligands that mediate cell–cell interactions and tight binding to the tumor extracellular matrix. When used as a coating material for nanoparticles, this membrane provides homologous recognition that enhances tumor penetration while sim-

Table 1 Size- or charge-transformable nanomedicine

Type	Nanoplatform	Stimuli	Size/charge change		Tumor	Ref.
			Initial	Final		
Size-transform	QDGelNPs (quantum dot gelatin nanoparticles)	MMP-2	~100 nm	~10 nm	HT-1080 fibrosarcoma xenograft model	Wong et al.[69]
	IDDHN	HAase	~264 nm	29–50 nm	4T1 breast cancer model	Hu et al.[13]
	BP-KLVFF-His6-PEG self-assembled nanoparticles	Acidic TME	~40 nm	Nanofiber	MCF-7 xenografts following NIR	Yang et al.[70]
	USMSN-NH2@LL-SP-C9	Acidic TME	~33 nm	~17 nm	4T1 breast cancer model	He et al.[14]
	PEG-TGA-NapFFKY@DOX self-assembled micelles	GSH	~192 nm	Nanofiber	A549 xenograft models	Guo et al.[71]
	Disulfide-crosslinked nanogel based nanoassemblies	GSH	150–250 nm	10–40 nm	CT26 colon cancer spheroids	Campea et al.[72]
Charge-transform	S(DGL)n@Apt	Hypoxia	Negative	Positive	Orthotopic PDAC	Chen et al.[73]
	Met@BF	Acidic TME	Negative	Positive	B16F10 cancer model	Wang et al.[74]
	HMSNs	Acidic TME	Negative	Positive	A549 cancer model	Liu et al.[75]
	CdSe/ZnS quantum dots with GGT-cleavable peptide	γ-GGT	Negative	Positive	GGT-positive cancer cells	Dai et al.[76]

ultaneously enabling immune evasion and prolonged circulation. Chen et al. reported cancer cell membrane–biomimetic nanoparticles (ICNPs) composed of an indocyanine green (ICG)–loaded PLGA core cloaked with a membrane shell derived from MCF-7 cells.[77] Benefiting from the preserved adhesion molecules such as EpCAM, N-cadherin, and galectin-3, ICNPs exhibited strong homologous targeting and efficient penetration in tumors. This coating reduced clearance by the liver and kidney, improved real-time imaging with dual fluorescence/photoacoustic modalities, and, under near-infrared irradiation, achieved complete ablation of xenografted tumors without relapse. These findings highlight cancer cell membrane functionalization as a powerful bio-inspired strategy to couple immune camouflage with deep tumor penetration.

In addition to leveraging membrane ligands, tumor penetration can also be enhanced through structural design. Nie et al. developed cancer cell membrane–coated nanoparticles with a yolk–shell structure (CCM@LM), in which a mesoporous silica–supported PEGylated liposome formed the yolk and was further cloaked with an MCF-7-derived membrane.[78] The yolk–shell architecture endowed the nanoparticles with moderate rigidity and the capacity to deform into an ellipsoidal shape during infiltration, facilitating rotation-mediated penetration through multicellular spheroids and tumor extracellular matrix. Moreover, CCM@LM entered cells via a membrane fusion pathway mimicking enveloped viruses, followed by efficient cytosolic trafficking and perinuclear accumulation of the PEGylated yolk. When co-loaded with doxorubicin and the PARP inhibitor mefuparib hydrochloride, CCM@LM achieved a 95% tumor inhibition rate at a relatively low dose, highlighting how biomimetic surface chemistry combined with structural flexibility can synergistically promote tumor penetration and therapeutic efficacy.

Red blood cell (RBC) membranes offer another bio-inspired strategy by transferring both immune-evasive markers and the intrinsic deformability of native erythrocytes. Miao et al. designed RBC membrane–camouflaged elastic nanoparticles (RBC-ENPs) composed of poly (ethylene glycol) diacrylate (PEGDA) hydrogel cores coated with natural RBC membranes.[15] This core–shell structure preserved essential surface proteins such as CD47 while enabling tunable mechanical elasticity that closely mimics the flexibility of dynamic erythrocytes. The deformable hydrogel core allowed RBC-ENPs to undergo reversible shape transitions under shear stress, resembling erythrocytes squeezing through narrow capillaries. This property facilitated efficient diffusion through the dense tumor extracellular matrix, leading to superior penetration in multicellular spheroids and enhanced tumor accumulation in vivo. Furthermore, the RBC coating minimized protein corona formation and opsonization, resulting in ultralong systemic circulation and reduced macrophage uptake. When loaded with doxorubicin, RBC-ENPs significantly outperformed PEGylated liposomes in inhibiting 4T1 breast tumors while maintaining high biocompatibility.

Exosome-inspired nanomaterials. Exosomes are cell-derived extracellular vesicles that naturally mediate intercellular communication by transferring proteins, lipids, and nucleic acids within the body.[79] Their lipid bilayer membranes are enriched with adhesion molecules, integrins, and surface glycoconjugates, which enable specific interactions with target cells and efficient navigation across complex biological barriers.[80] Inspired by these properties, exosome-mimetic nanomaterials have been engineered to recapitulate their biocompatibility, immune-evasive capacity, and homotypic targeting functions. In the context of solid tumors, such bio-inspired designs enhance penetration by promoting transcytosis across endothelial and stromal barriers, reducing clearance by the mononuclear phagocyte system, and facilitating diffusion through the dense extracellular matrix. Consequently, exosome-inspired nanocarriers provide a powerful strategy to overcome

the intrinsic transport limitations of conventional nanomedicines and achieve deep and uniform tumor penetration.

One of the earliest demonstrations of this concept was reported by Jang *et al.*, who developed exosome-mimetic nanovesicles (NVs) through serial extrusion of monocytes and macrophages.[81] These NVs preserved key plasma membrane proteins such as LFA-1, which mediate adhesion to endothelial cell adhesion molecules (CAMs), thereby enabling selective accumulation at tumor-associated vasculature. When loaded with doxorubicin, NVs achieved efficient vascular targeting and deep tumor penetration, significantly enhancing antitumor efficacy in syngeneic models while minimizing systemic toxicity. Importantly, enzymatic removal of membrane proteins abrogated these effects, highlighting the essential role of preserved surface ligands in tumor-specific penetration.

Building on this foundation, Wang *et al.* designed an exosome membrane–coated programmable paclitaxel prodrug nanoplatform (EMPCs) that co-delivered a ROS-responsive paclitaxel-linoleic acid conjugate with cucurbitacin B.[82] The exosome membrane, derived from MDA-MB-231 breast cancer cells, retained key surface proteins such as CD44 and CD47, which enabled homotypic recognition and immune evasion. This biomimetic surface allowed EMPCs to bind tightly to both circulating tumor cells and primary tumors, facilitating prolonged circulation, efficient accumulation, and notably deeper tumor penetration compared with uncoated nanoparticles. Once internalized, cucurbitacin B amplified intracellular ROS to trigger sequential activation of the paclitaxel prodrug, while concurrently suppressing FAK/MMP signaling to block metastasis. The exosome coating not only improved tissue infiltration by promoting adhesion-mediated transcytosis through dense tumor regions but also enhanced diffusion across 3D spheroids and orthotopic tumor masses. *In vivo*, EMPCs achieved deep intratumoral distribution, efficient circulating tumor cell clearance, and robust inhibition of both primary and metastatic tumor growth.

Similarly, Niu *et al.* developed a biomimetic hybrid delivery system by integrating natural grapefruit-derived extracellular vesicles (EVs) with doxorubicin-loaded, heparin-based nanoparticles (DNs) to overcome the blood–brain barrier (BBB) and enhance drug penetration in glioma.[83] The EV coating retained transmembrane proteins such as CD81 and TSG101, enabling receptor-mediated transcytosis and membrane fusion with brain endothelial cells, while the heparin-based DNs provided pH-sensitive, controlled drug release in acidic tumor microenvironments. This design achieved a fourfold increase in drug loading compared to conventional EV encapsulation and markedly enhanced penetration across the BBB and into glioma tissues. In intracranial tumor models, the EV-DN hybrids exhibited prolonged systemic circulation, high tumor accumulation, and potent anti-glioma efficacy, highlighting the promise of biomimetic EV-based systems for deep tumor penetration and brain-targeted chemotherapy.

More recently, Bang *et al.* introduced exosome-like vesicles (ELVs) that integrate three essential exosomal components (cholesterol, aquaporin-1, and anionic lipids) into synthetic lipid nanoparticles to replicate the superior diffusion and tissue-penetrating characteristics of natural exosomes.[84] Cholesterol increased membrane rigidity and colloidal stability, aquaporin-1 enhanced deformability for navigating narrow ECM pores, and anionic lipids reduced electrostatic trapping within negatively charged ECM networks. This synergistic composition markedly improved diffusion efficiency compared with conventional liposomes, resulting in uniform nanoparticle distribution throughout tumor tissues. In 4T1 breast tumor models, ELVs occupied over 95% of the tumor area, whereas liposomes remained limited to about 65%, confirming that the exosome-inspired design enabled more extensive and homogeneous tumor penetration. When loaded with doxorubicin, these ELVs exhibited significantly deeper intratumoral penetration and stronger antitumor effects than standard liposomal formulations, underscoring how exosome-inspired lipid nanocarriers can effectively overcome matrix barriers for enhanced tumor penetration.

Collectively, these studies highlight the versatility of exosome-inspired strategies in addressing multiple barriers to drug delivery, ranging from vascular adhesion and endothelial transcytosis to extracellular matrix diffusion and even metastasis control. By leveraging the intrinsic biological functionalities of exosomal membranes, such platforms not only improve tumor penetration but also broaden the therapeutic potential of nanomedicines across diverse cancer models. Continued optimization of these bioinspired designs is expected to accelerate their translation toward clinically viable therapies for solid tumors.

3.3. Targeting extracellular matrix

The ECM of solid tumors undergoes extensive remodeling during tumor progression and becomes enriched with fibrillar collagens, hyaluronic acid, proteoglycans, and cross-linking enzymes secreted mainly by cancer-associated fibroblasts and stellate cells. This desmoplastic network increases matrix stiffness and solid stress, elevates interstitial fluid pressure, compresses intratumoral blood vessels, and narrows interstitial pores, all of which restrict perfusion and convective transport. As a result, nanomedicines that rely on the EPR effect often accumulate near blood vessels but fail to reach poorly perfused tumor cores. To overcome these biophysical barriers, various strategies have been developed to modulate the extracellular matrix.

ECM-degrading agents and enzymes. Targeting the ECM therefore represents a pivotal strategy to overcome the biophysical barriers that restrict nanomedicine penetration. Beyond approaches that normalize stromal synthesis or modulate mechanical stresses, direct degradation of key ECM components such as collagen, hyaluronic acid, and proteoglycans can create transient transport channels, reduce interstitial pressure, and restore vascular perfusion. These interventions not only facilitate nanoparticle diffusion into hypoxic tumor cores but also improve the infiltration of therapeutic antibodies and immune effector cells. Such effects are most achieved using ECM-degrading agents and enzymes, which

have been extensively explored as adjuvants to enhance drug delivery efficacy.

As a representative example, Lee *et al.* developed a dual-responsive nanocomplex (NOTAb) that co-delivers a ROS-sensitive nitric oxide (NO) prodrug with αPD-L1 antibody.[85] Within the tumor microenvironment, elevated ROS levels trigger NO release, which activates MMPs and induces collagen degradation, thereby relieving the physical ECM barrier. Subsequently, the acidic pH of the tumor core facilitates the release of αPD-L1, enabling deeper penetration of both the antibody and cytotoxic T lymphocytes. This strategy not only enhanced intratumoral distribution of αPD-L1 but also promoted T cell infiltration, reprogrammed the immunosuppressive microenvironment, and resulted in robust tumor regression with prolonged survival in murine colon cancer models.

Building on this concept, Chen *et al.* reported a sequential delivery approach to address the dense desmoplastic stroma in pancreatic ductal adenocarcinoma (PDAC).[86] In this system, liposomes loaded with the NO donor *S*-nitroso-*N*-acetylpenicillamine (Lip-SNAP) were first delivered to pancreatic stellate cells, effectively inhibiting TGF-β1 signaling and suppressing the production of α-SMA, fibronectin, and collagen. This NO-induced stromal depletion substantially reduced matrix density and hydraulic resistance, thereby facilitating the penetration of subsequently administered gemcitabine-loaded liposomes (Lip-GEM). In both subcutaneous and orthotopic PDAC models, the combination of Lip-SNAP pretreatment and Lip-GEM therapy achieved superior drug distribution, enhanced tumor regression, and prolonged survival compared to monotherapy. These findings establish NO-mediated stromal modulation as a promising avenue for overcoming ECM barriers and improving nanomedicine delivery in stroma-rich tumors.

Beyond small-molecule or gaseous mediators, enzymatic degradation strategies provide a more direct and potent means of dismantling the stromal barrier. For instance, Li *et al.* engineered sono-activatable semiconducting polymer nanoreshapers (SPN$_{DN}$H) functionalized with HAase to degrade hyaluronic acid in the pancreatic tumor microenvironment.[87] The HAase-mediated ECM remodeling facilitated nanoparticle enrichment and T cell infiltration, while concomitant H$_2$S release alleviated hypoxia, thereby amplifying sonodynamic therapy (SDT)–induced immunogenic cell death. Under ultrasound activation, SPN$_{DN}$H also enabled on-demand release of an IDO inhibitor, effectively reversing immunosuppressive signaling. This multifaceted remodeling strategy resulted in nearly complete inhibition of orthotopic pancreatic tumor growth and suppression of metastasis, highlighting the translational promise of enzyme-based ECM modulation for deep tumor penetration and immunotherapy.

In a complementary approach, Ikeda-Imafuku *et al.* developed a collagen type IV–binding peptide–hyaluronic acid conjugate for targeted delivery of bromelain (C4BP-HA-Bro) into tumor stroma.[88] The C4BP peptide was selected for its strong affinity to the extracellular matrix of triple-negative breast cancer tissue, allowing specific accumulation of the conjugate

in tumors while minimizing off-target distribution. This construct preserved the enzymatic activity of bromelain after conjugation and efficiently degraded fibrillar ECM components, shortening collagen fibers and enhancing matrix porosity. As a result, pretreatment with C4BP-HA-Bro markedly improved the intratumoral distribution and therapeutic efficacy of liposomal doxorubicin, while avoiding the systemic toxicity observed with free bromelain. These results demonstrate that selective stromal targeting combined with localized enzymatic degradation can safely and effectively potentiate nanomedicine penetration within dense tumor tissues.

In another representative study, Wang *et al.* developed collagenase-conjugated transcytosis nanoparticles (Col-TNPs) designed to enhance the intracellular transport of nanomedicines across the dense stroma of pancreatic adenocarcinoma.[89] Upon accumulation in the tumor microenvironment, Col-TNPs released collagenase in response to acidic pH, effectively degrading collagen fibers that otherwise hindered nanoparticle internalization and cell-to-cell transcytosis. This enzymatic remodeling facilitated active transcytosis of cationized nanoparticles into avascular tumor regions, thereby achieving homogeneous intratumoral distribution and significantly augmenting the radiosensitization efficacy of pancreatic tumors. Importantly, Col-TNP treatment exhibited minimal systemic toxicity while markedly improving radiotherapeutic outcomes.

Collectively, these studies highlight how ECM-degrading agents and enzymes can act in complementary ways, either by chemically loosening the stromal network or by enzymatically dismantling key structural components, to relieve biophysical barriers. Such strategies not only unlock transport pathways for nanoparticles but also potentiate immunotherapy, chemotherapy, and radiotherapy by enabling deeper and more uniform tumor penetration.

ECM-binding peptides. In addition to degrading or remodeling the extracellular matrix, an alternative approach involves exploiting peptides that specifically bind to overexpressed ECM components in tumors. These ECM-binding peptides recognize tumor-restricted motifs that are minimally expressed in normal tissues but highly abundant in malignant stroma. By anchoring therapeutic or imaging agents to these stable ECM scaffolds, they enhance local drug retention, promote deeper tissue penetration through multivalent interactions, and facilitate the recruitment of immune effector cells.

Among the diverse classes of tumor-penetrating peptides, iRGD (CRGDKGPDC) represents one of the most extensively characterized and validated prototypes, with broad applicability across various solid tumor models.[90] This peptide initially binds to αv integrins overexpressed on tumor endothelium and stroma, and upon proteolytic cleavage, the exposed C-end rule (CendR) motif engages neuropilin-1 to trigger active transcytosis and deep tissue penetration. By converting perivascular retention into trans-tissue transport, iRGD enhances both vascular permeability and interstitial diffusion, thereby promoting uniform intratumoral distribution of therapeutics. For instance, Wang *et al.* conjugated iRGD to hybrid nanoparticles co-loaded with the photosensitizer indocyanine

Table 2 Nanomedicine design strategies targeting the ECM for deep tumor penetration

Strategy	Nanoplatform	Encapsulated material	Target	Mechanism for deep penetration	Ref.
ECM-degradation	NOTAb	αPD-L1 Ab	Collagen	ROS-mediated NO release	Lee et al.[85]
	Liposome	NO donor Lip-SNAP, gemcitabine Lip-GEM	Collagen, fibronectin, α-SMA	NO inhibits TGF-β1 and reduce ECM synthesis	Chen et al.[86]
	SPNDNH + HAase	NLG919, H₂S donor	Hyaluronic acid-rich ECM	HAase-mediated HA degradation	Li et al.[87]
	C4BP-HA-Bro	Bromelain, doxorubicin	Collagen IV, fibrillar ECM	ECM-binding peptide localization of bromelain and collagen degradation	Ikeda-Imafuku et al.[88]
	Col-TNPs	Collagenase, cationic NPs	Collagen fibers	Acidic pH induces collagenase release and collagen degradation	Li et al.[89]
ECM-binding	iRGD-conjugated hybrid PLGA/lipid NP	ICG, TPZ	αv integrin, neuropilin-1	iRGD-mediated αv integrin/neuropilin-1 binding–induced transcytosis and ECM penetration	Wang et al.[91]
	PL1-functionalized NP	Proapoptotic peptide	FN-EDB, TNC-C	PL1-driven tumor-stroma homing and multivalent ECM anchoring	Lingasamy et al.[93]
	C-DVM	Doxorubicin, vinorelbine	Fibronectin	CREKA-based fibronectin targeting–induced micelle concentration	Gong et al.[94]

green (ICG) and the hypoxia-activated prodrug tirapazamine (TPZ).[91] The iRGD-modified nanoparticles penetrated more efficiently into 3D spheroids and orthotopic breast tumors, enabling synergistic photodynamic and hypoxia-activated chemotherapy that effectively suppressed both primary tumor growth and metastasis with minimal systemic toxicity.

Beyond iRGD, other ECM-binding peptides have been identified to broaden tumor selectivity and overcome stromal heterogeneity. A notable example is the bispecific peptide PL1 (PPRRGLIKLKTS), which simultaneously binds to both fibronectin extra domain B (FN-EDB) and tenascin-C C domain (TNC-C), two ECM isoforms abundantly expressed in malignant tissues but largely absent in normal stroma.[92] Lingasamy et al. demonstrated that PL1-functionalized nanoparticles, including iron oxide nanoworms and silver nanoparticles, selectively homed to glioblastoma and prostate carcinoma xenografts, where they colocalized with FN-EDB and TNC-C deposition and accumulated deep within tumor parenchyma beyond the perivascular region.[93] This enhanced infiltration was attributed to the dual engagement of ECM receptors, which increased nanoparticle retention and transvascular diffusion. When conjugated to therapeutic payloads such as proapoptotic peptides, PL1-targeted nanocarriers significantly suppressed tumor growth and prolonged survival in glioblastoma models, outperforming non-targeted controls while sparing healthy tissues. These findings underscore the potential of bispecific ECM-binding ligands to improve nanoparticle accumulation, tumor penetration, and therapeutic efficacy in heterogeneous solid tumors.

An additional study by Gong et al. utilized an ECM-binding peptide–based approach by developing fibronectin-targeted dual-acting micelles (C-DVM) functionalized with the CREKA peptide to selectively accumulate in metastatic breast cancer foci.[94] CREKA binding to fibrin–fibronectin complexes within the tumor stroma facilitated strong adhesion to metastatic sites and improved micelle diffusion throughout the dense extracellular matrix, enabling more uniform intratumoral drug distribution. By co-encapsulating doxorubicin and vinorelbine within stable PEGylated micelles, this platform combined DNA synthesis inhibition and microtubule disruption while maintaining prolonged systemic circulation. In 4T1 breast cancer models, C-DVM achieved efficient drug codelivery, deep tumor penetration, and a 90% reduction in metastatic foci compared to conventional formulations, demonstrating the promise of ECM-targeting peptides in enhancing both delivery and therapeutic efficacy.

Taken together, these studies illustrate how ECM-binding peptides, from integrin- and neuropilin-targeting iRGD to bispecific ligands such as PL1 and fibronectin-specific CREKA, provide versatile tools to overcome stromal barriers and achieve selective drug enrichment in both primary and metastatic tumors. By converting the ECM from a barrier into a therapeutic anchor, peptide-guided strategies hold significant promise for advancing nanomedicine penetration and improving outcomes in otherwise treatment-resistant cancers (Table 2).

4. External stimuli and pharmacological modulators for enhanced tumor penetration

Exogenous physical fields and biochemical adjuvants can be layered onto nanomedicine design to actively overcome vascular and stromal resistances that restrict particle motion to perivascular margins. By converting field energy or small molecule cues into mechanical forces, transient barrier loosening, or guided transport, these approaches increase the length scale of dispersion from vessels into the parenchyma and improve the uniformity of intratumoral exposure.

4.1. Physical modalities

Ultrasound. Ultrasound can transiently enhance convective and diffusive transport within tumors by promoting endo-

thelial junction opening, lowering interstitial resistance, and generating acoustic microstreaming that propels nanosystems through dense extracellular matrix.

A representative study by Lee *et al.* demonstrated that pulsed high-intensity focused ultrasound (pHIFU) could non-invasively remodel the dense ECM of A549 lung carcinoma tumors, thereby facilitating nanoparticle penetration.[95] Using glycol chitosan nanoparticles (Cy5.5-CNPs) as a model system, the authors showed that ECM-rich tumors with high collagen and hyaluronan levels markedly restricted intratumoral accumulation compared to ECM-poor tumors. While intratumoral injection of collagenase or hyaluronidase improved nanoparticle delivery, pHIFU exposure at low power (5 W cm^{-2}) achieved similar ECM remodeling effects without tissue ablation. pHIFU treatment increased blood flow, reduced collagen density, and enhanced nanoparticle penetration into tumor cores, resulting in a 2.5-fold improvement in tumor targeting compared to untreated controls. These findings establish pulsed-HIFU as a clinically relevant, noninvasive strategy to disrupt stromal barriers and improve the delivery efficiency of nanomedicines in ECM-rich solid tumors.

A subsequent study by Li *et al.* further demonstrated how ultrasound can be leveraged to potentiate deep penetration in chemoresistant tumors.[96] They engineered pullulan-all-*trans*-retinal (PR) nanoparticles encapsulating doxorubicin-loaded nanodiamonds (DOX-NDs/PR), which exhibited high dispersity, pH-responsive release, and synergistic cytotoxicity from both doxorubicin and retinoic acid. Upon ultrasound exposure, endothelial tight junctions were transiently opened, facilitating vascular extravasation and deep penetration of the nanodiamond-based carriers. *In vivo*, ultrasound combined with DOX-NDs/PR enhanced doxorubicin accumulation up to 17.3% of the injected dose within tumors, significantly suppressed growth of both doxorubicin-sensitive and resistant HepG2 xenografts, and prolonged survival while minimizing systemic toxicity. This work highlights ultrasound-triggered vascular permeabilization as a powerful strategy to overcome drug efflux and intratumoral transport barriers in refractory cancers.

A further refinement was reported by Li *et al.*, who designed a redox-sensitive core-crosslinked nanosystem (NDX–CCS) composed of doxorubicin-loaded nanodiamonds coated with a diselenide-crosslinked pullulan shell.[97] This design improved monodispersity, prolonged systemic stability, and enabled tumor-specific drug release in response to the redox microenvironment. When combined with ultrasound irradiation, NDX–CCS exhibited enhanced vascular permeabilization and deeper tumor penetration, leading to significantly higher intratumoral accumulation and superior tumor growth inhibition in HepG2 xenografts compared to non-crosslinked controls or free doxorubicin. Importantly, this strategy achieved strong therapeutic efficacy with minimal systemic toxicity, underscoring the translational potential of integrating ultrasound-triggered vascular modulation with redox-sensitive nanocarriers for deep tumor penetration.

In summary, these ultrasound-based strategies demonstrate how mechanical and biochemical effects induced by ultra-

sound irradiation can be harnessed to overcome stromal barriers. By facilitating both vascular permeabilization and active intratumoral transport, ultrasound offers a versatile and clinically relevant external stimulus to enhance nanomedicine penetration and therapeutic efficacy.

Magnetic fields. Magnetic fields provide a bio-orthogonal means to manipulate nanomedicines *in vivo*, as biological tissues are essentially transparent to magnetic flux. When functionalized with superparamagnetic iron oxide or other magnetic domains, nanocarriers can be guided by external fields to accumulate at tumor sites. Beyond passive deposition through the EPR effect, magnetic actuation supplies body forces that bias extravasation and actively propel carriers through tortuous extracellular matrix, thereby extending penetration beyond the short diffusion-limited length scales that typically confine nanoparticles to perivascular regions. This capability makes magnetic targeting an attractive approach to overcome both vascular and stromal transport barriers in solid tumors.

A representative example was reported by Liu *et al.*, who developed a dual-magnet platform generating oppositely polarized static fields to enhance the delivery of superparamagnetic iron oxide nanoparticle (SPION) micelles into tumors.[98] Unlike conventional single-magnet systems, which exhibit a rapid decay of field strength with distance and are thus limited to superficial tissues, this device established a constant radial gradient that actively drove nanocarriers outward into the tumor mass. In murine 4T1 breast tumor models, the system achieved a five-fold increase in penetration depth and a three-fold increase in total intratumoral accumulation compared to EPR alone. Histological analysis confirmed that SPION micelles dispersed significantly further from blood vessels under the dual-magnet configuration than with single-magnet or control conditions, underscoring the ability of magnetophoresis to overcome interstitial resistance and enable deeper tumor penetration.

Along similar lines, Zhu *et al.* engineered large deformable polymeric nanocarriers (^{DA}T-PPE$_{D\&F}$) integrating ferrimagnetic nanocubes and a pH-sensitive TAT peptide.[99] Under magnetic actuation, these nanocarriers underwent efficient extravasation and actively penetrated into deep tumor tissue, surpassing the limitations typically faced by rigid nanoparticles of similar size. The deformability of the polyphosphoester core facilitated active navigation through dense extracellular matrix, while the acidic tumor microenvironment reactivated the masked TAT peptide to further promote tumor cell uptake. As a result, doxorubicin-loaded ^{DA}T-PPE$_{D\&F}$ achieved broad intratumoral delivery and nearly complete tumor suppression in breast and colon cancer models, underscoring the translational promise of magnetically actuated deformable nanocarriers for deep tumor penetration.

In further advancement, Jang *et al.* constructed an 8-magnet device arranged in an annular Halbach array, which generated a strong and constant radial magnetic field gradient to actively propel magnetic nanocarriers into tumor tissue.[100] Using chlorin e6−coated cobalt-doped iron oxide nanoclusters,

this approach achieved nearly a seven-fold increase in nano-particle migration through porous matrices compared to the prior two-magnet setup. In orthotopic 4T1 breast tumor models, the optimized magnetic field markedly enhanced intratumoral accumulation and, importantly, deep tissue penetration of nanoclusters, thereby significantly improving the therapeutic efficacy of photodynamic therapy.

These findings underscore how rational engineering of magnetic field architecture can overcome diffusion-limited transport and drive nanoparticles far beyond perivascular regions. By leveraging enhanced magnetic propulsion, tumor penetration was substantially amplified, positioning magnetically actuated delivery systems as a promising strategy to improve the therapeutic index of nanomedicines.

Photothermal. Photothermal activation has been increasingly incorporated into nanomedicine design as a minimally invasive strategy to enhance intratumoral transport.[118] Upon irradiation, photothermal agents convert light energy into localized heat, which can transiently remodel stromal barriers or modulate carrier properties *in situ*.

Yu *et al.* developed a mesoporous polydopamine (MPDA) nanoplatform co-loaded with bromelain and the immune adjuvant R848 (M@B/R) to enhance photothermal immunotherapy for osteosarcoma.[101] Upon NIR irradiation, the MPDA core converted light into localized heat, simultaneously inducing immunogenic cell death and activating bromelain for extracellular matrix degradation. This dual action not only facilitated dendritic cell maturation and cytotoxic T lymphocyte infiltration but also cleared collagen barriers that otherwise restricted nanoparticle and immune cell transport. *In vivo*, the combination of PTT, bromelain-mediated ECM clearance, and R848-driven immune activation led to potent tumor regression and extended survival in osteosarcoma-bearing mice, underscoring how photothermal-triggered ECM remodeling can significantly improve tumor penetration and therapeutic efficacy.

Cancer-associated fibroblasts (CAFs) are a dominant stromal component in desmoplastic tumors, where they continuously secrete collagen, hyaluronic acid, and cross-linking enzymes that stiffen the extracellular matrix and elevate interstitial pressure.[102,103] This pathological remodeling restricts nanoparticle transport, confining most nanomedicines to perivascular zones. To overcome this barrier, Nicolás-Boluda *et al.* developed a photothermal strategy to selectively deplete CAFs and remodel the stiff stromal architecture in desmoplastic cholangiocarcinoma. They engineered hybrid gold-decorated iron oxide nanoflowers (GIONFs) capable of efficient near-infrared–induced mild hyperthermia.[104] The nanoparticles preferentially accumulated in αSMA-positive fibroblasts, and repeated photothermal treatments led to selective CAF ablation, matrix softening, and vascular decompression without damaging tumor parenchyma. This mechanical normalization significantly enhanced nanoparticle diffusion and drug distribution throughout the tumor mass, converting a rigid, chemoresistant stroma into a more permeable microenvironment. *In vivo*, three rounds of GIONF-mediated therapy induced marked tumor softening, improved chemotherapeutic delivery, and complete tumor regression in most treated mice, highlighting the potential of CAF-targeted photothermal modulation to improve nanomedicine penetration and therapeutic efficacy in desmoplastic tumors.

Radiotherapy. Radiation has been shown to transiently remodel the tumor microenvironment in ways that favor nanoparticle penetration. By disrupting tight junctions, widening intercellular spaces, and modulating intratumoral fluid dynamics, radiation reduces physical resistance within tumors and permits deeper movement of nanomedicines beyond perivascular zones. This barrier-relieving effect can be further amplified when radiation is combined with other physical modulators such as heat.

Stapleton *et al.* demonstrated that a single dose of radiation or mild hyperthermia substantially enhanced the tumor uptake and distribution of liposomal nanomedicines in high–interstitial fluid pressure breast cancer models.[105] Radiation pretreatment reduced interstitial fluid pressure and induced spatiotemporal fluctuations in fluid transport, which allowed nanoparticles to reach the tumor core rather than remaining confined to peripheral regions. When administered prior to liposomal doxorubicin (Doxil), radiation significantly improved intratumoral exposure, delayed tumor growth, and extended survival compared to drug alone, underscoring its potential as an adjuvant for enhancing nanotherapeutic penetration.

In a complementary study, Hargrove *et al.* developed mesoporous silica nanoparticles (MSNs) loaded with the therapeutic radionuclide holmium-166 (^{166}Ho) for the treatment of ovarian peritoneal metastases.[106] Following intraperitoneal administration, non-radioactive ^{165}Ho-MSNs primarily accumulated at tumor surfaces with limited penetration. In contrast, radioactive ^{166}Ho-MSNs exhibited markedly deeper distribution throughout tumor tissues, with penetration depths extending up to 800–900 μm within 7 days. This radiation-induced penetration was attributed to localized ionizing radiation disrupting stromal collagen and expanding interstitial spaces, thereby facilitating nanoparticle migration beyond superficial zones. Dosimetry analysis further confirmed that this deeper penetration enabled more uniform absorbed dose distribution across tumor tissue. *In vivo*, fractionated dosing of ^{166}Ho-MSNs significantly suppressed tumor progression, prolonged survival, and reduced ascites formation compared with controls, demonstrating that internal radiation can actively remodel tumor barriers to promote deeper nanomedicine penetration.

Radiation can also be harnessed in combination with stimuli-responsive nanomaterials to further potentiate tumor penetration. Fu *et al.* designed a TME-responsive "small-on-large" MoS_2/HfO_2-dextran (M/H-D) nanoradiosensitizer that undergoes disassembly upon NIR irradiation and enzymatic degradation, releasing ultrasmall HfO_2 nanoparticles with markedly improved diffusivity.[107] This disintegration not only facilitated deep intratumoral penetration but also enhanced radiosensitization by overcoming the poor cellular internalization of inert HfO_2. In addition, the photothermal conversion

of MoS_2 alleviated hypoxia and boosted ROS production, thereby synergizing with radiotherapy to achieve pronounced DNA damage and tumor regression *in vivo*. Importantly, this strategy allowed real-time monitoring of penetration and hypoxia relief *via* CT and photoacoustic imaging, underscoring the translational potential of stimuli-responsive radiosensitizers.

Taken together, these studies highlight that radiation does more than directly damage tumor DNA. It can actively reshape the tumor microenvironment and cooperate with smart nanoplatforms to enhance intratumoral transport. By combining physical disruption of tumor barriers with stimuli-responsive designs, radiation-assisted nanomedicines provide a powerful route to overcome the bottleneck of limited tumor penetration and improve therapeutic efficacy.

4.2. Vascular modulation strategies

The abnormal architecture and dysfunction of tumor vasculature impose a major barrier to nanomedicine transport, often resulting in heterogeneous perfusion and confinement of nanoparticles near perivascular regions. Vascular modulation strategies aim to transiently improve perfusion or normalize vessel function, thereby enhancing extravasation and interstitial delivery of therapeutics.

Vasodilators. Pharmacological vasodilators reduce vascular resistance by relaxing smooth muscle in vessel walls, thereby expanding lumen diameter and improving blood flow. In tumors, this transient increase in perfusion can lower interstitial fluid pressure and enlarge the effective surface area for nanoparticle extravasation, enabling more homogeneous penetration into poorly perfused regions. By directly modulating vascular tone, vasodilators can act as powerful adjuvants to enhance the delivery efficiency of nanomedicines.

As an illustrative example, Woeppel *et al.* engineered a conducting polymer–based nanoparticle system using poly(ethylenedioxythiophene) (PEDOT) doped with sulfonated mesoporous silica nanoparticles to load and release the vasodilator sodium nitroprusside (NaNP) *in vivo*.[108] Electrical stimulation triggered on-demand release of NaNP, leading to significant dilation of cortical blood vessels in mice as visualized by two-photon microscopy. This localized and controllable vasodilation increased vessel diameter in a size-dependent manner, demonstrating that targeted vasodilator delivery can dynamically modulate perfusion. While developed in the context of neurovascular modulation, this strategy underscores the broader potential of vasodilator-assisted nanomedicine to improve vascular transport and facilitate deeper tumor penetration.

In addition to electrically controlled vasodilator release, tumor microenvironment–responsive strategies have been developed to achieve localized vasodilation and further improve nanoparticle penetration. Zhang *et al.* introduced a tumor-acidity–responsive platform in which sildenafil, a clinically used vasodilator, was encapsulated into cisplatin-loaded polymeric micelles.[109] In the acidic tumor microenvironment, sildenafil underwent protonation and was selectively released,

inducing localized vasodilation without systemic hypotension. This vascular remodeling significantly enlarged vessel perimeters, enhanced permeability, and thereby facilitated deeper nanoparticle penetration and higher cisplatin accumulation within tumors. In melanoma models, the co-loaded nanoparticles demonstrated greater therapeutic efficacy and prolonged survival compared to cisplatin alone, highlighting tumor-acidity–triggered sildenafil release as a simple yet effective strategy to improve nanomedicine penetration and outcomes.

In line with these strategies, Chen *et al.* developed a liposomal delivery system incorporating the vasodilator hydralazine (HDZ), a clinically used antihypertensive agent, to overcome stromal barriers in desmoplastic tumors.[110] HDZ-liposomes expanded tumor vasculature and attenuated fibroblast activation and collagen deposition, thereby softening the dense stroma. Importantly, HDZ-liposome pretreatment significantly increased nanoparticle accumulation and interstitial penetration, with fluorescent liposomes detected up to 60–75 μm away from tumor vessels, approximately three times deeper than in untreated controls. This enhanced diffusion was accompanied by improved oxygenation and reduced hypoxia-inducible factor (HIF)-1α expression, indicating improved perfusion and lower interstitial pressure. When combined with doxorubicin-loaded liposomes, the sequential regimen achieved pronounced tumor inhibition even in large desmoplastic melanomas exceeding 400 mm^3, demonstrating that vasodilator-induced vascular remodeling can effectively enhance nanoparticle penetration and therapeutic outcomes.

Angiogenesis modulators. Abnormal angiogenesis produces highly disorganized and leaky tumor vessels, which elevates interstitial fluid pressure, collapses functional perfusion, and restricts nanoparticle penetration to perivascular regions. Modulating angiogenesis through vascular normalization can transiently restore structural integrity and functional flow, reduce interstitial fluid pressure, and establish pressure gradients that drive more effective transvascular and interstitial transport. This approach has emerged as a promising strategy to convert heterogeneous and inefficient vasculature into a more physiologically balanced network that supports deeper and more uniform nanomedicine delivery.

Chauhan *et al.* provided direct experimental evidence for this concept by blocking VEGF receptor-2 with the antibody DC101 in mammary tumor models.[111] Vascular normalization improved the penetration of small nanoparticles of around 12 nm by up to threefold, whereas delivery of larger nanoparticles in the 60 to 125 nm range was not enhanced and, in some cases, even hindered. Intravital microscopy confirmed that normalization decreased vessel pore size heterogeneity, reduced interstitial fluid pressure, and promoted convective transport, thereby defining a transient normalization window that favored smaller nanomedicines. Importantly, combination studies showed that normalization enhanced the therapeutic efficacy of approximately 10 nm Abraxane but not 100 nm Doxil, highlighting the size-dependent nature of this strategy.

Ha *et al.* expanded this concept by designing a pH-sensitive liposomal nanoplatform, OD_PSL@AKB, that co-delivers oxygen and the VE-PTP inhibitor razuprotafib (AKB-9778) to simultaneously alleviate hypoxia and normalize tumor vasculature.[112] In the acidic tumor microenvironment, OD_PSL@AKB rapidly released its payload, restoring VE-cadherin expression, reducing VEGF secretion, and stabilizing endothelial junctions through Tie-2 pathway activation. Oxygen supplementation further relieved hypoxia, suppressing HIF-1α signaling and thereby interrupting the vicious cycle of abnormal angiogenesis. This dual action markedly improved vascular perfusion and permeability, resulting in enhanced nanoparticle penetration and greater therapeutic efficacy in multiple tumor models. Collectively, these results highlight how rationally engineered angiogenesis modulators can restore functional vasculature and create a transient therapeutic window that favors deeper and more uniform intratumoral nanomedicine distribution.

5. Conclusion and future perspectives

Tumor penetration of nanomedicines arises from a multifactorial interplay of intrinsic physicochemical parameters, including particle size, surface charge, deformability, morphology, and material composition, which collectively dictate pharmacokinetics and tissue transport. Each parameter provides specific functional advantages at distinct stages of the delivery cascade yet inherently compromises performance at others, creating persistent design trade-offs. To reconcile these conflicts, recent advances have yielded stimuli-responsive and transformable nanoplatforms capable of *in situ* adaptation, bioinspired surface architectures that confer immune evasion and tumor-selective affinity, and extracellular matrix (ECM)-targeted systems that convert stromal barriers into active transport pathways. In addition, vascular normalization and external stimuli-assisted modulation have emerged as complementary strategies that promote homogeneous nanoparticle distribution beyond perivascular regions.

Translating these innovations from preclinical validation to clinical application, however, requires overcoming significant barriers that extend beyond benchtop optimization. A major limitation in current research is that many penetration-enhancing strategies are validated primarily in murine or spheroid models, which fail to fully recapitulate the extensive interpatient and intra-tumoral heterogeneity found in human cancers. Consequently, nanomedicines optimized for uniform animal models often encounter unanticipated transport barriers in clinical settings; this disconnect is a primary driver behind the high attrition rates observed in past clinical trials. Furthermore, the transition to clinical use is heavily impeded by challenges related to scale-up, regulatory feasibility, and commercial viability. The complex multi-component nature of modern nanoplatforms complicates quality control and reproducibility, making mass production costly. Moreover, regulatory approval pathways for these multifunctional systems remain ill-defined, and their cost-effectiveness relative to standard-of-care therapies is rarely addressed at early stages. These factors, together with market adoption hurdles, represent major commercialization barriers that must be considered to enable real-world implementation. Therefore, future development must address these translational realities early in the design phase, ensuring that sophisticated systems are not only effective but also manufacturable and compliant with safety guidelines.

Crucially, the lack of consensus on optimal nanoparticle design rules reflects not only methodological heterogeneity but, more fundamentally, the dominant influence of tumor-specific biology over physicochemical parameters. Across the literature, conflicting conclusions regarding the ideal size, shape, and surface charge for tumor accumulation and penetration persist because nanoparticle performance is evaluated in biologically distinct models that differ markedly in cellular architecture, endocytic capacity, extracellular matrix density, stromal organization, and vascular functionality. Under such conditions, incremental variations in nanoparticle design are frequently overshadowed by cancer-specific transport barriers and uptake mechanisms, rendering design principles derived from a single tumor model inherently context-dependent.[113–115] Addressing this challenge will require systematic, biology-driven comparisons that decouple intrinsic nanoparticle properties from tumor microenvironmental effects by rigorously controlling material composition and biological variables. Only through such approaches can robust, generalizable, and clinically relevant design rules for tumor penetration be established. Notably, recent studies employing three-dimensional tumor models and standardized nanoparticle libraries, in which size, shape, and surface charge are systematically varied while material composition and biological context are held constant, exemplify this emerging effort toward establishing more robust design rules.[116]

Looking ahead, context-responsive nanomedicines that integrate size or charge transformation with bio-inspired coatings and vascular or stromal normalization represent one of the most promising strategies for achieving clinically meaningful outcomes. Critically, these advances will require co-optimization frameworks in which intrinsic nanoparticle properties and extrinsic microenvironment-modulating interventions are designed in a coordinated, stage-specific manner rather than in isolation. Such systems-level approaches acknowledge that transport efficiency, cellular uptake, and intratumoral distribution emerge from dynamic interactions between material properties and tumor biology. The future of this field will depend on the ability to tailor designs to patient-specific tumor microenvironments, guided by biomarkers of stromal density, vascular function, acidity, or enzyme activity. However, the widespread clinical realization of patient-specific and context-responsive nanomedicines remains constrained by significant translational impediments. Key hurdles include the rigorous validation and standardization of predictive bio-

markers, the temporal evolution of tumor heterogeneity, and the seamless integration of complex adaptive platforms into established clinical protocols. Consequently, a critical examination of these logistical constraints is imperative to ensure a realistic assessment of the near-term feasibility of personalized nanomedicine strategies. Convergence with artificial intelligence for predictive modeling, real-time imaging for adaptive dosing, and combination therapies will likely accelerate clinical translation. Ultimately, advancing tumor penetration will require integrative nanomedicine platforms that couple adaptive physicochemical properties with tumor microenvironment normalization and patient-specific design, translating pre-clinical efficacy into clinically predictable and durable therapeutic responses.

Collectively, this review synthesizes two central conclusions regarding the determinants of tumor penetration. First, intrinsic physicochemical optimization alone is insufficient due to inevitable design trade-offs between systemic circulation and deep tissue transport, necessitating the adoption of stimuli-responsive and transformable nanoplatforms that dynamically adapt to the microenvironment. Second, effective penetration often requires overcoming dominant biological barriers, notably dense stroma and abnormal vasculature, through extrinsic strategies including physical modulation, enzymatic remodeling, and pharmacological normalization, rather than relying solely on passive nanoparticle accumulation. Ultimately, the future of nanomedicine lies in the co-optimization of these adaptive intrinsic designs with extrinsic microenvironment-modulating interventions to achieve clinically meaningful therapeutic outcomes.

Author contributions

The manuscript was written through the contributions of all authors. All authors have approved the final version of the manuscript. Dongwon Shin: conceptualization, data curation, visualization, writing – original draft. Jiwoong Choi: conceptualization, data curation, visualization, writing – original draft. Byeongmin Park: data curation, visualization. Sun Hwa Kim: resources, funding acquisition, project administration, writing – original draft, writing – review & editing. Man Kyu Shim: conceptualization, resources, supervision, funding acquisition, project administration, writing-original draft, writing-review & editing.

Conflicts of interest

The authors declare no conflict of interest.

Abbreviation

BBB	Blood–brain barrier
CAFs	Cancer-associated fibroblasts
CAMs	Cell adhesion molecules
CendR	C-end rule
DOPC	Dioleoylphosphatidylcholine
Doxil	Liposomal doxorubicin
DPPC	Dipalmitoylphosphatidylcholine
ECM	Extracellular matrix
ELVs	Exosome-like vesicles
EPR	Enhanced permeability and retention
EVs	Extracellular vesicles
FN-EDB	Fibronectin extra domain B
GEM	Gemcitabine
GGT	γ-Glutamyl transpeptidase
GMP	Good manufacturing practice
GSH	Glutathione
HDZ	Hydralazine
HIF	Hypoxia-inducible factor
ICG	Indocyanine green
IDD	Indocyanine green/doxorubicin
iRGD	CRGDKGPDC; tumor-penetrating peptide
M/H-D	MoS_2/HfO_2-dextran
MMP-2	Matrix metalloproteinase-2
MPDA	Mesoporous polydopamine
MPS	Mononuclear phagocyte system
MSNs	Mesoporous silica nanoparticles
NaNP	Sodium nitroprusside
NO	Nitric oxide
NVs	Nanovesicles
PDAC	Pancreatic ductal adenocarcinoma
PEDOT	Poly(ethylenedioxythiophene)
PEG	Poly(ethylene glycol)
PEGDA	Poly(ethylene glycol) diacrylate
pHIFU	Pulsed high-intensity focused ultrasound
PR	Pullulan-all-*trans*-retinal
QDs	Quantum dots
RBC	Red blood cell
RES	Reticulorendothelial system
ROS	Reactive oxygen species
SDT	Sonodynamic therapy
SPION	Superparamagnetic iron oxide nanoparticle
TME	Tumor microenvironment
TNC-C	Tenasein-C C domain
TPZ	Tirapazamine
VEGF	Vascular endothelial growth factor
VE-PTP	Vascular endothelial-protein tyrosine phosphatase

Data availability

No primary research results, software or code have been included, and no new data was generated or analyzed as part of this review.

Acknowledgements

References

1 W. J. Stark, P. R. Stoessel, W. Wohlleben and A. Hafner, *Chem. Soc. Rev.*, 2015, **44**, 5793–5805.

2 M. De, P. S. Ghosh and V. M. Rotello, *Adv. Mater.*, 2008, **20**, 4225–4241.

3 L. A. Lane, X. Qian, A. M. Smith and S. Nie, *Annu. Rev. Phys. Chem.*, 2015, **66**, 521–547.

4 L. Tang, X. Yang, Q. Yin, K. Cai, H. Wang, I. Chaudhury, C. Yao, Q. Zhou, M. Kwon and J. A. Hartman, *Proc. Natl. Acad. Sci. U. S. A.*, 2014, **111**, 15344–15349.

5 J. Fang, W. Islam and H. Maeda, *Adv. Drug Delivery Rev.*, 2020, **157**, 142–160.

6 S. Lim, J. Park, M. K. Shim, W. Um, H. Y. Yoon, J. H. Ryu, D.-K. Lim and K. Kim, *Theranostics*, 2019, **9**, 7906.

7 H. Maeda, J. Wu, T. Sawa, Y. Matsumura and K. Hori, *J. Controlled Release*, 2000, **65**, 271–284.

8 S. Yang, I.-C. Sun, H. S. Hwang, M. K. Shim, H. Y. Yoon and K. Kim, *J. Mater. Chem. B*, 2021, **9**, 3983–4001.

9 X. Duan and Y. Li, *Small*, 2013, **9**, 1521–1532.

10 J. Ding, J. Chen, L. Gao, Z. Jiang, Y. Zhang, M. Li, Q. Xiao, S. S. Lee and X. Chen, *Nano Today*, 2019, **29**, 100800.

11 Q. Sun, T. Ojha, F. Kiessling, T. Lammers and Y. Shi, *Biomacromolecules*, 2017, **18**, 1449–1459.

12 M. Souri, A. Golzaryan and M. Soltani, *Eur. J. Pharm. Biopharm.*, 2024, **199**, 114310.

13 C. Hu, X. L. Cun, S. B. Ruan, R. Liu, W. Xiao, X. T. Yang, Y. Y. Yang, C. Y. Yang and H. L. Gao, *Biomaterials*, 2018, **168**, 64–75.

14 Y. J. He, X. Y. Fan, X. Z. Wu, T. S. Hu, F. F. Zhou, S. W. Tan, B. T. Chen, A. Q. Pan, S. Q. Liang and H. Xu, *Nanoscale*, 2022, **14**, 1271–1284.

15 Y. Q. Miao, Y. T. Yang, L. M. Guo, M. S. Chen, X. Zhou, Y. G. Zhao, D. Nie, Y. Gan and X. X. Zhang, *ACS Nano*, 2022, **16**, 6527–6540.

16 M. Binnewies, E. W. Roberts, K. Kersten, V. Chan, D. F. Fearon, M. Merad, L. M. Coussens, D. I. Gabrilovich, S. Ostrand-Rosenberg, C. C. Hedrick, R. H. Vonderheide, M. J. Pittet, R. K. Jain, W. P. Zou, T. K. Howcroft, E. C. Woodhouse, R. A. Weinberg and M. F. Krummel, *Nat. Med.*, 2018, **24**, 541–550.

17 J. L. Chitty and T. R. Cox, *Trends Cancer*, 2025, **11**, 839–849.

18 Q. Sun, Z. Zhou, N. Qiu and Y. Shen, *Adv. Mater.*, 2017, **29**, 1606628.

19 S. Liu, Z. Ren, M. Yan, W. Ye and Y. Hu, *Biomaterials*, 2025, **321**, 123315.

20 M. K. Shim, S. Yang, I.-C. Sun and K. Kim, *Adv. Drug Delivery Rev.*, 2022, **183**, 114177.

21 B. Alallam, H. Choukaife, S. Seyam, V. Lim and M. Alfatama, *Gels*, 2023, **9**, 115.

22 D. Fan, Y. Cao, M. Cao, Y. Wang, Y. Cao and T. Gong, *Signal Transduction Targeted Ther.*, 2023, **8**, 293.

23 J. Q. Wang, W. W. Mao, L. L. Lock, J. B. Tang, M. H. Sui, W. L. Sun, H. G. Cui, D. Xu and Y. Q. Shen, *ACS Nano*, 2015, **9**, 7195–7206.

24 M. K. Shim, J. Park, H. Y. Yoon, S. Lee, W. Um, J.-H. Kim, S.-W. Kang, J.-W. Seo, S.-W. Hyun and J. H. Park, *J. Controlled Release*, 2019, **294**, 376–389.

25 J. Choi, M. K. Shim, S. Yang, H. S. Hwang, H. Cho, J. Kim, W. S. Yun, Y. Moon, J. Kim and H. Y. Yoon, *ACS Nano*, 2021, **15**, 12086–12098.

26 H. Cabral, Y. Matsumoto, K. Mizuno, Q. Chen, M. Murakami, M. Kimura, Y. Terada, M. R. Kano, K. Miyazono, M. Uesaka, N. Nishiyama and K. Kataoka, *Nat. Nanotechnol.*, 2011, **6**, 815–823.

27 H. S. Choi, W. Liu, P. Misra, E. Tanaka, J. P. Zimmer, B. I. Ipe, M. G. Bawendi and J. V. Frangioni, *Nat. Biotechnol.*, 2007, **25**, 1165–1170.

28 F. Alexis, E. Pridgen, L. K. Molnar and O. C. Farokhzad, *Mol. Pharmaceutics*, 2008, **5**, 505–515.

29 H.-X. Wang, Z.-Q. Zuo, J.-Z. Du, Y.-C. Wang, R. Sun, Z.-T. Cao, X.-D. Ye, J.-L. Wang, K. W. Leong and J. Wang, *Nano Today*, 2016, **11**, 133–144.

30 Q. Q. Lu, H. Y. Yu, T. C. Zhao, G. J. Zhu and X. M. Li, *Nanoscale*, 2023, **15**, 13202–13223.

31 C. B. He, Y. P. Hu, L. C. Yin, C. Tang and C. H. Yin, *Biomaterials*, 2010, **31**, 3657–3666.

32 G. Y. Wang, Y. Y. Chen, P. Wang, Y. F. Wang, H. Hong, Y. L. Li, J. C. Qian, Y. Yuan, B. Yu and C. S. Liu, *Acta Biomater.*, 2016, **29**, 248–260.

33 X. C. He, Y. Y. Yang, Y. L. Han, C. Y. Cao, Z. B. Zhang, L. X. Li, C. L. Xiao, H. Guo, L. Wang, L. C. Han, Z. G. Qu, N. Liu, S. Han and F. Xu, *Proc. Natl. Acad. Sci. U. S. A.*, 2023, **120**, e2209260120.

34 T. Stylianopoulos, M. Z. Poh, N. Insin, M. G. Bawendi, D. Fukumura, L. L. Munn and R. K. Jain, *Biophys. J.*, 2010, **99**, 1342–1349.

35 C. C. Fleischer and C. K. Payne, *J. Phys. Chem. B*, 2014, **118**, 14017–14026.

36 M. P. Monopoli, C. Åberg, A. Salvati and K. A. Dawson, *Nat. Nanotechnol.*, 2012, **7**, 779–786.

37 S. Schöttler, K. Landfester and V. Mailänder, *Angew. Chem., Int. Ed.*, 2016, **55**, 8806–8815.

38 Z. Li, X. L. Yang and Z. F. Li, *Chem. Mater.*, 2024, **36**, 1041–1053.

39 L. Zhang, Z. Q. Cao, Y. T. Li, J. R. Ella-Menye, T. Bai and S. Y. Jiang, *ACS Nano*, 2012, **6**, 6681–6686.

40 Z. Li, Y. B. Zhu, H. W. Zeng, C. Wang, C. Xu, Q. Wang, H. M. Wang, S. Y. Li, J. T. Chen, C. Xiao, X. L. Yang and Z. F. Li, *Nat. Commun.*, 2023, **14**, 4524.

41 L. Y. Zhang, H. M. Chen, E. Lindberg, J. Xie, M. Becton and X. Q. Wang, *J. Phys. Chem. B*, 2021, **125**, 1529–1529.

42 S. de Weerd, X. Y. Ma, Z. Zohali, L. L. Oudejans, E. Kyrloglou, M. C. A. Stuart, W. H. Roos, J. J. Schuringa and A. Salvati, *Adv. Healthcare Mater.*, 2025, **14**, 2500667.

43 P. Gurnani, C. Sanchez-Cano, H. Xandri-Monje, J. L. Zhang, S. H. Ellacott, E. D. H. Mansfield, M. Hartlieb, R. Dallmann and S. Perrier, *Small*, 2022, **18**, 2203070.

44 X. D. Shen, D. Y. Pan, Q. Y. Gong, Z. W. Gu and K. Luo, *Bioact. Mater.*, 2024, **32**, 445–472.

45 C. Kinnear, T. L. Moore, L. Rodriguez-Lorenzo, B. Rothen-Rutishauser and A. Petri-Fink, *Chem. Rev.*, 2017, **117**, 11476–11521.

46 A. Jahangiri-Manesh, M. Mousazadeh, S. Taji, A. Bahmani, A. Zarepour, A. Zarrabi, E. Sharifi and M. Azimzadeh, *Pharmaceutics*, 2022, **14**, 664.

47 S. Raghuram, Y. Mackeyev, J. Symons, Y. Zahra, V. Gonzalez, K. K. Mahadevan, K. I. Requejo, A. Liopo, P. Derry, E. Zubarev, O. Sahin, J. B. K. Kim, P. K. Singh, S. H. Cho and S. Krishnan, *Biomaterials*, 2022, **291**, 121887.

48 A. O. Elzoghby, O. Samir, A. Soliman, S. Solomevich, M. Z. Yu, A. Schwendeman and M. L. Nasr, *Nano Today*, 2023, **53**, 102026.

49 I. S. Pires, A. Hostetler, G. Covarrubias, I. S. Carlo, J. R. Suggs, B. J. Kim, A. J. Pickering, E. Gordon, D. J. Irvine and P. T. Hammond, *Adv. Mater.*, 2024, **36**, 2408307.

50 L. García-Hevia, R. Soltani, J. González, O. Chaloin, C. Ménard-Moyon, A. Bianco and M. L. Fanarraga, *Bioact. Mater.*, 2024, **34**, 237–247.

51 V. Rastogi, P. Yadav, S. S. Bhattacharya, A. K. Mishra, N. Verma, A. Verma and J. K. Pandit, *J. Drug Delivery*, 2014, **2014**, 670815.

52 P. S. Zangabad, M. Karimi, F. Mehdizadeh, H. Malekzad, A. Ghasemi, S. Bahrami, H. Zare, M. Moghoofei, A. Hekmatmanesh and M. R. Hamblin, *Nanoscale*, 2017, **9**, 1356–1392.

53 S. Bhaskar and S. Lim, *NPG Asia Mater.*, 2017, **9**, e371.

54 T. H. Kim, C. W. Mount, B. W. Dulken, J. Ramos, C. J. Fu, H. A. Khant, W. Chiu, W. R. Gombotz and S. H. Pun, *Mol. Pharmaceutics*, 2012, **9**, 135–143.

55 M. Ghezzi, S. Pescina, C. Padula, P. Santi, E. Del Favero, L. Cantù and S. Nicoli, *J. Controlled Release*, 2021, **332**, 312–336.

56 S. Shukla, F. J. Eber, A. S. Nagarajan, N. A. DiFranco, N. Schmidt, A. M. Wen, S. Eiben, R. M. Twyman, C. Wege and N. F. Steinmetz, *Adv. Healthc. Mater.*, 2015, **4**, 874–882.

57 M. U. Munir, *Cancers*, 2022, **14**, 2904.

58 B. R. Smith, P. Kempen, D. Bouley, A. Xu, Z. Liu, N. Melosh, H. J. Dai, R. Sinclair and S. S. Gambhir, *Nano Lett.*, 2012, **12**, 3369–3377.

59 X. Yi, X. H. Shi and H. J. Gao, *Phys. Rev. Lett.*, 2011, **107**, 199902.

60 S. L. Zhang, H. J. Gao and G. Bao, *ACS Nano*, 2015, **9**, 8655–8671.

61 S. Chakraborty, M. Doktorova, T. R. Molugu, F. A. Heberle, H. L. Scott, B. Dzikovski, M. Nagao, L. R. Stingaciu, R. F. Standaert, F. N. Barrera, J. Katsaras, G. Khelashvili, M. F. Brown and R. Ashkar, *Proc. Natl. Acad. Sci. U. S. A.*, 2020, **117**, 21896–21905.

62 Y. Takechi-Haraya, K. Sakai-Kato, Y. Abe, T. Kawanishi, H. Okuda and Y. Goda, *Langmuir*, 2016, **32**, 6074–6082.

63 B. Park, J. Choi, J.-H. Lee, Y. Kim, W. Lee, A. Lee, I.-C. Sun, H. Y. Yoon, Y. Kim and S. H. Kim, *Signal Transduction Targeted Ther.*, 2025, **10**, 310.

64 J. Choi, B. Park, J. Y. Park, D. Shin, S. Lee, H. Y. Yoon, K. Kim, S. H. Kim, Y. Kim and Y. Yang, *Adv. Mater.*, 2024, **36**, 2405475.

65 M. K. Shim, H. Y. Yoon, S. Lee, M. K. Jo, J. Park, J.-H. Kim, S. Y. Jeong, I. C. Kwon and K. Kim, *Sci. Rep.*, 2017, **7**, 1–15.

66 Y. Jang, J. Choi, B. Park, J. Y. Park, J.-H. Lee, J. Goo, D. Shin, S. H. Kim, Y. Kim and H. K. Song, *Acta Pharm. Sin. B*, 2025, 4886–4899.

67 Y. Moon, M. K. Shim, J. Choi, S. Yang, J. Kim, W. S. Yun, H. Cho, J. Y. Park, Y. Kim and J.-K. Seong, *Theranostics*, 2022, **12**, 1999.

68 M. K. Shim, H. Y. Yoon, J. H. Ryu, H. Koo, S. Lee, J. H. Park, J. H. Kim, S. Lee, M. G. Pomper and I. C. Kwon, *Angew. Chem.*, 2016, **128**, 14918–14923.

69 C. Wong, T. Stylianopoulos, J. A. Cui, J. Martin, V. P. Chauhan, W. Jiang, Z. Popovic, R. K. Jain, M. G. Bawendi and D. Fukumura, *Proc. Natl. Acad. Sci. U. S. A.*, 2011, **108**, 2426–2431.

70 P. P. Yang, Q. Luo, G. B. Qi, Y. J. Gao, B. N. Li, J. P. Zhang, L. Wang and H. Wang, *Adv. Mater.*, 2017, **29**, 1605869.

71 W. W. Guo, Z. T. Zhang, Q. C. Wei, Y. Zhou, M. T. Lin, J. J. Chen, T. T. Wang, N. N. Guo, X. C. Zhong, Y. Y. Lu, Q. Y. Yang, M. Han and J. Q. Gaon, *Biomacromolecules*, 2020, **21**, 444–453.

72 M. A. Campea, A. Lofts, F. Xu, M. Yeganeh, M. Kostashuk and T. Hoare, *ACS Appl. Mater. Interfaces*, 2023, **15**, 25324–25338.

73 H. Y. Chen, Q. Guo, Y. C. Chu, C. Li, Y. W. Zhang, P. X. Liu, Z. H. Zhao, Y. Wang, Y. F. Luo, Z. Zhou, T. Y. Zhang, H. L. Song, X. W. Li, C. F. Li, B. Y. Su, H. Y. You, T. Sun and C. Jiang, *Biomaterials*, 2022, **287**, 121599.

74 Y. Wang, Q. S. Tang, R. Q. Wu, S. Y. Yang, Z. S. Geng, P. He, X. D. Li, Q. F. Chen and X. L. Liang, *ACS Nano*, 2024, **18**, 6314–6332.

75 J. J. Liu, X. M. Guo, Z. Luo, J. X. Zhang, M. H. Li and K. Y. Cai, *Nanoscale*, 2018, **10**, 13737–13750.

76 Q. J. Dai, Z. Du, L. H. Jing, R. C. Zhang and W. Tang, *ACS Appl. Mater. Interfaces*, 2024, **16**, 6208–6220.

77 Z. Chen, P. F. Zhao, Z. Y. Luo, M. B. Zheng, H. Tian, P. Gong, G. H. Gao, H. Pan, L. L. Liu, A. Q. Ma, H. D. Cui, Y. F. Ma and L. T. Cai, *ACS Nano*, 2016, **10**, 10049–10057.

78 D. Nie, Z. Dai, J. L. Li, Y. W. Yang, Z. Y. Xi, J. Wang, W. Zhang, K. Qian, S. Y. Guo, C. L. Zhu, R. Wang, Y. M. Li, M. R. Yu, X. X. Zhang, X. H. Shi and Y. Gan, *Nano Lett.*, 2020, **20**, 936–946.

79 H. I. Kim, J. Park, Y. Zhu, X. Y. Wang, Y. H. Han and D. Zhang, *Exp. Mol. Med.*, 2024, **56**, 836–849.

80 M. A. Kumar, S. K. Baba, H. Q. Sadida, S. A. Marzooqi, J. Jerobin, F. H. Altemani, N. Algehainy, M. A. Alanazi, A. B. Abou-Samra, R. Kumar, A. S. A. Akil, M. A. Macha, R. Mir and A. A. Bhat, *Signal Transduction Targeted Ther.*, 2024, **9**, 27.

81 S. C. Jang, O. Y. Kim, C. M. Yoon, D. S. Choi, T. Y. Roh, J. Park, J. Nilsson, J. Lötvall, Y. K. Kim and Y. S. Gho, *ACS Nano*, 2014, **8**, 1073–1073.

82 K. Y. Wang, H. Ye, X. B. Zhang, X. Wang, B. Yang, C. Luo, Z. Q. Zhao, J. Zhao, Q. Lu, H. T. Zhang, Q. M. Kan, Y. J. Wang, Z. G. He and J. Sun, *Biomaterials*, 2020, **257**, 120224.

83 W. B. Niu, Q. Xiao, X. J. Wang, J. Q. Zhu, J. H. Li, X. M. Liang, Y. M. Peng, C. T. Wu, R. J. Lu, Y. Pan, J. M. Luo, X. X. Zhong, H. Q. He, Z. L. Rong, J. B. Fan and Y. Wang, *Nano Lett.*, 2021, **21**, 1484–1492.

84 S. Bang, B. Park, J. C. Park, H. Jin, J. S. Shim, J. Koo, K. H. Lee, M. K. Shim and H. Kim, *ACS Nano*, 2025, **19**, 8882–8894.

85 J. Lee, H. Cho, J. Kim, J. Lim, Y. Kang and W. J. Kim, *J. Controlled Release*, 2025, **381**, 113576.

86 X. H. Chen, F. Jia, Y. Z. Li, Y. Y. Deng, Y. Huang, W. F. Liu, Q. Jin and J. Ji, *Biomaterials*, 2020, **246**, 119999.

87 M. Li, Y. Liu, Y. J. Zhang, N. Y. Yu and J. C. Li, *Adv. Sci.*, 2023, **10**, 2305150.

88 M. Ikeda-Imafuku, Y. S. Gao, S. Shaha, L. L. W. Wang, K. S. Park, M. Nakajima, O. Adebowale and S. Mitragotri, *J. Controlled Release*, 2022, **352**, 1093–1103.

89 L. Wang, J. X. Dou, W. Jiang, Q. Wang, H. Liu, Y. C. Wang and Y. Liu, *Nano Lett.*, 2022, **22**, 6877–6887.

90 X. S. Liu, J. H. Jiang, Y. Ji, J. Q. Lu, R. Chan and H. Meng, *Mol. Syst. Des. Eng.*, 2017, **2**, 370–379.

91 Y. Z. Wang, Y. Xie, J. Li, Z. H. Peng, Y. Sheinin, J. P. Zhou and D. Oupicky, *ACS Nano*, 2019, **13**, 4855–4855.

92 P. Lingasamy, K. Posnograjeva, S. Kopanchuk, A. Tobi, A. Rinken, I. J. General, E. K. Asciutto and T. Teesalu, *Pharmaceutics*, 2021, **13**, 1365.

93 P. Lingasamy, A. Tobi, M. Haugas, H. Hunt, P. Paiste, T. Asser, T. Rätsep, V. R. Kotamraju, R. Bjerkvig and T. Teesalu, *Biomaterials*, 2019, **219**, 119373.

94 Z. R. Gong, M. Chen, Q. S. Ren, X. L. Yue and Z. F. Dai, *Signal Transduction Targeted Ther.*, 2020, **5**, 12.

95 S. Lee, H. Han, H. Koo, J. H. Na, H. Y. Yoon, K. E. Lee, H. Lee, H. Kim, I. C. Kwon and K. Kim, *J. Controlled Release*, 2017, **263**, 68–78.

96 H. N. Li, M. Ma, J. N. Zhang, W. Hou, H. R. Chen, D. P. Zeng and Z. B. Wang, *ACS Appl. Mater. Interfaces*, 2019, **11**, 20341–20349.

97 M. X. Li, Q. Y. Li, W. Hou, J. N. Zhang, H. M. Ye, H. A. Li, D. P. Zeng and J. Bai, *RSC Adv.*, 2020, **10**, 15252–15263.

98 J. F. Liu, Z. Y. Lan, C. Ferrari, J. M. Stein, E. Higbee-Dempsey, L. Yan, A. Amirshaghaghi, Z. L. Cheng, D. Issadore and A. Tsourkas, *ACS Nano*, 2020, **14**, 142–152.

99 Y. Q. Zhu, Y. H. Song, Z. Y. Cao, L. Dong, Y. Lu, X. Z. Yang and J. Wang, *Adv. Funct. Mater.*, 2021, **31**, 2008208.

100 B. Jang, A. Amirshaghaghi, J. Choi, J. Miller, D. A. Issadore, T. M. Busch, Z. L. Cheng and A. Tsourkas, *ACS Nano*, 2025, **19**, 1794–1808.

101 Z. L. Yu, Z. Q. Gan, W. Wu, X. J. Sun, X. F. Cheng, C. Chen, B. H. Cao, Z. Y. Sun and J. W. Tian, *ACS Appl. Mater. Interfaces*, 2024, **16**, 67225–67234.

102 W. Q. Shen, P. A. Yao, W. J. Li, C. J. Gu, T. Gao, Y. Cao, Z. Wang, R. J. Pei and C. E. Xing, *J. Mater. Chem. B*, 2023, **11**, 1871–1880.

103 D. K. Yang, J. Liu, H. Qian and Q. Zhuang, *Exp. Mol. Med.*, 2023, **55**, 1322–1332.

104 A. Nicolás-Boluda, J. Vaquero, G. Laurent, G. Renault, R. Bazzi, E. Donnadieu, S. Roux, L. Fouassier and F. Gazeau, *ACS Nano*, 2020, **14**, 5738–5753.

105 S. Stapleton, M. Dunne, M. Milosevic, C. W. Tran, M. J. Gold, A. Vedadi, T. D. Mckee, P. S. Ohashi, C. Allen and D. A. Jaffray, *ACS Nano*, 2018, **12**, 7583–7600.

106 D. Hargrove, S. Ranjbar, M. Darji, S. Nam, R. J. Dawson, S. Katugampola, X. H. Lin, A. Brown, N. Carrasco-Rojas, C. Goodwin, R. W. Howell, W. E. Bolch, M. Jay, A. Salner and X. L. Lu, *Int. J. Pharm.*, 2025, **669**, 125071.

107 W. H. Fu, X. Zhang, L. Q. Mei, R. Y. Zhou, W. Y. Yin, Q. Wang, Z. J. Gu and Y. L. Zhao, *ACS Nano*, 2020, **14**, 10001–10017.

108 K. M. Woeppel, D. D. Krahe, E. M. Robbins, A. L. Vazquez and X. T. Cui, *Adv. Healthc. Mater.*, 2024, **13**, 2301221.

109 P. Zhang, Y. Zhang, X. Y. Ding, C. S. Xiao and X. S. Chen, *Biomater. Sci.*, 2020, **8**, 3052–3062.

110 Y. Z. Chen, W. T. Song, L. M. Shen, N. S. Qiu, M. Y. Hu, Y. Liu, Q. Liu and L. Huang, *ACS Nano*, 2019, **13**, 1751–1763.

111 V. P. Chauhan, T. Stylianopoulos, J. D. Martin, Z. Popovic, O. Chen, W. S. Kamoun, M. G. Bawendi, D. Fukumura and R. K. Jain, *Nat. Nanotechnol.*, 2012, **7**, 383–388.

112 H. Ha, Y. Choi, N. H. Kim, J. Kim, J. Jang, T. H. R. Niepa, M. Tanaka, H. Y. Lee and J. Choi, *Biomater. Res.*, 2025, **29**, 0144.

113 S. Behzadi, V. Serpooshan, W. Tao, M. A. Hamaly, M. Y. Alkawareek, E. C. Dreaden, D. Brown, A. M. Alkilany, O. C. Farokhzad and M. Mahmoudi, *Chem. Soc. Rev.*, 2017, **46**, 4218–4244.

114 T. dos Santos, J. Varela, I. Lynch, A. Salvati and K. A. Dawson, *PLoS One*, 2011, **6**, e24438.

115 C. Cortez-Jugo, E. Czuba-Wojnilowicz, A. Tan and F. Caruso, *Adv. Healthc. Mater.*, 2021, **10**, 2100574.

116 P. Cybulski, M. Bravo, J. J. K. Chen, I. Van Zundert, S. Krzyzowska, F. Taemaitree, H. Uji-i, J. Hofkens, S. Rocha and B. Fortuni, *Front. Cell Dev. Biol.*, 2025, **12**, 1520078.

117 B. Park, J. Choi, J.-H. Lee, Y. Kim, W. Lee, A. Lee, I.-C. Sun, H. Y. Yoon, Y. Kim, S. H. Kim, Y. Yang, K. Kim, J. Park and M. K. Shim, *Signal Transduction Targeted Ther.*, 2025, **10**(1), 310.

118 J. Choi, B. Park, J. Y. Park, D. Shin, S. Lee, H. Y. Yoon, K. Kim, S. H. Kim, Y. Kim, Y. Yang and M. K. Shim, *Adv. Mater.*, 2024, **36**(38), 2405475.